Validation Report for CAM OLP
OLP version: olp10b9

Diego A. Cesarsky
diego.cesarsky@mpe.mpg.de

March 2002

Max–Planck–Institut für extraterrestrische Physik, Garching

Version 0.4

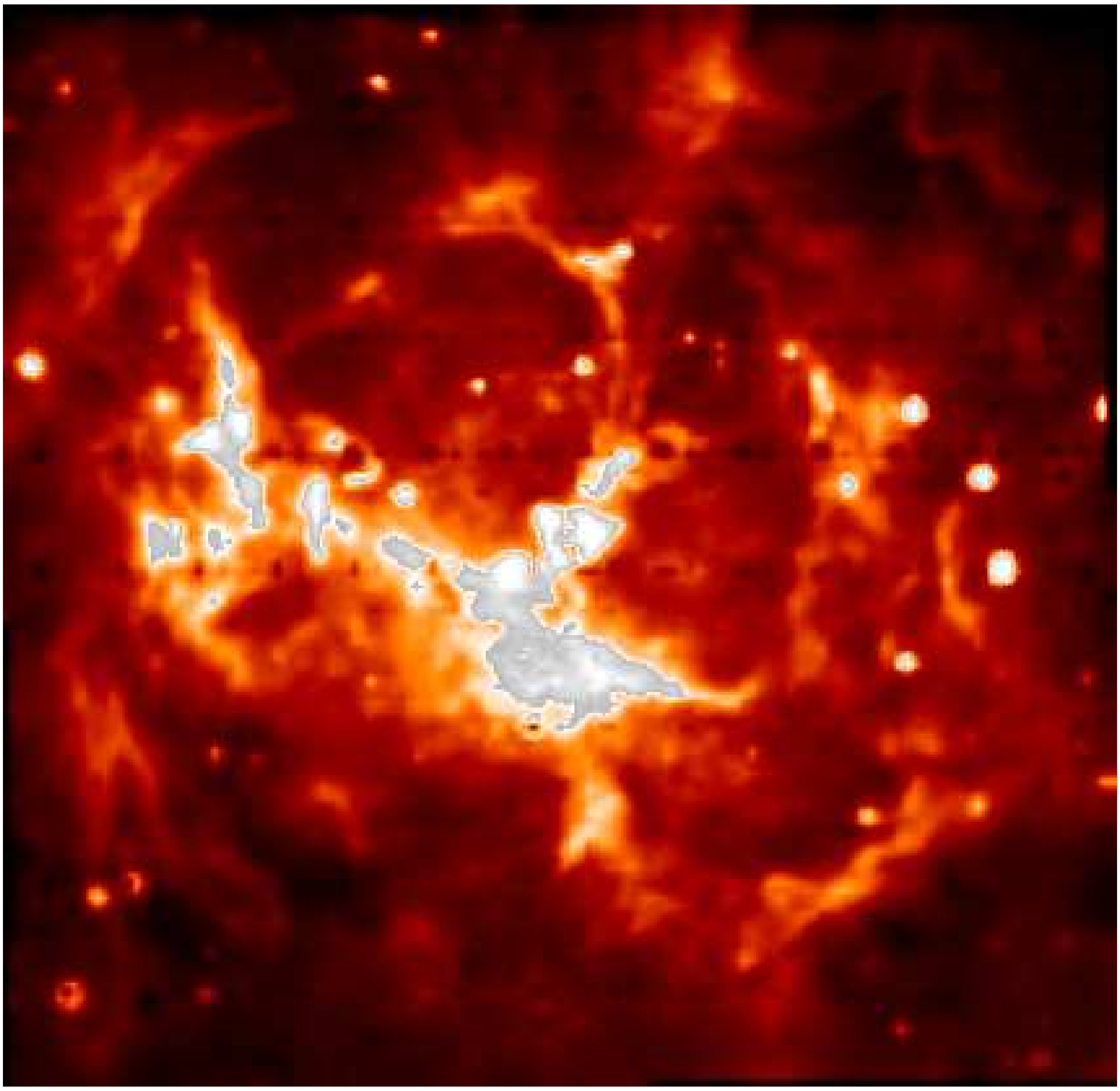

Figure 1: Map of M20 as seen by olp10b9

Contents

1 Introduction **5**

2 Change Record for OLP Version 10b9 **6**

2.1 SCREWs on CAM's OLP 6

2.1.1 Implemented SCREWs on SPC 6

2.1.2 Implemented SCREWs on AAC 6

2.2 SPRs on CAM's OLP 6

2.2.1 Implemented SPRs on SPC 6

2.2.2 Implemented SPRs on AAC 6

3 Comments on some major implemented SCREWs/SPRs **7**
3.1 Improved CSTA and CISP generation 7
3.2 LW detector transient corrections 7
3.3 New Point Source Detection algorithm 9

4 SPRs and SCREWs not closed for the "Legacy Archive" OLP **12**
4.1 Open SPRs 12
4.1.1 Notes to Table 2 12
4.2 Open SCREWs 18
4.2.1 Notes to the open SCREWs 18

5 Photometric accuracy of calibration stars **19**
5.1 HIC67485 - Plots and Tables 21
5.2 HIC69713 - Plots and Tables 23
5.3 HIC70218 - Plots and Tables 24
5.4 HIC73005 - Plots and Tables 26
5.5 HIC77277 - Plots and Tables 28
5.6 HIC85317 - Plots and Tables 30
5.7 HIC94376 - Plots and Tables 32
5.8 HIC94890 - Plots and Tables 35

6 Point source extraction and transient corrector **38**
6.1 Point source extraction: OLP vs. manual reduction 39

7 Photometric accuracy: conclusions **40**
7.1 Important note regarding HIC-star observations 41

8 Caveats for olp10b9 products **42**
8.1 First processing level 43
8.1.1 CSTA files 43
8.1.2 IIPH files 44
8.2 Second processing level 44
8.2.1 CISP/CPSP files 44
8.3 Third processing level 45
8.3.1 CCIM files 48
8.3.2 CMAP products 48
8.3.3 CMOS products 49
8.3.4 CPSL 50
8.3.5 CSSP files 51
8.3.6 CUFF 51
8.3.7 CJAM and CGLL files 51

A Figures for Section 6 **52**

1 Introduction

This is the Validation Report for the "legacy" version of the Off Line Processing (OLP): the data products that will populate the ISO archive will be generated by this version of OLP. For the validation report of this last version of the OLP software, I have at some places referred to statements from previous Validation Reports to give an idea of the progress made since earlier version of the pipeline.

The next statement is taken *verbatim* from the OLP version 9.0 report:

As several times stated in the POPS meetings, the main goal for CAM OLP Version 9.5 is

(1) Implementation of the Fouks-Schubert correction for LW observations, including delivery of its own CAL–G file

(2) A new algorithm to generate CAM's revolution–wide Continuous Status History File (CCSH), and the TDT–wide CSTA files.

(3) A new algorithm to generate as many SPCs records as number of readouts

(4) Close a number of SPRs and SCREWs applicable to SPC and AAC

This version of OLP incorporates the Fouks–Schubert correction code and the use of the recent Variable Dark CAL–G file. Not planned at the time the above statement was written, was the introduction of a new algorithm for Point Source detection, SPR3553. The need became obvious after realizing that most point sources reported by AAC were assigned a Flux generally 10-25% lower than the expected Flux and, in many cases, the old algorithm found bogus "point sources" in regions of high illumination gradient,see 3.3.

No changes have been introduced for the handling of the SW detector, other than the improvements introduced by the newer pointing corrections and the new point source detection algorithm.

The list of test cases used to establish this report is given in Appendix A.

Table 1: Scientific Validation of OLP AOT Processing, Second trimester 2001

AOT	**Submode**	**Valid since OLP**	**Plans for OLP 10**
CAM01	Staring observations	V4	See note 1
	Raster mode (low or no redundancy)	V4	See note 2
	Raster mode (redundant)	V4	See note 3
CAM03	Beam Switching	V4	See note 4
CAM04	CVF observations	V4	See note 5
CAM05	Polarisation observations	V7	See note 6

Note 1 No major upgrade currently planned (other than improved CAL-G)

Note 2 No major upgrade currently planned (other than improved CAL-G)

Note 3 Use of a SLICE–like post-processor driven by CAM_BPG (also improved CAL-G)

Note 4 No major upgrade currently planned (other than improved CAL-G)

Note 5 No major upgrade currently planned (other than improved CAL-G)

Note 6 No major upgrade currently planned (other than improved CAL-G)

2 Change Record for OLP Version 10b9

For an overview of the changed modules (subroutines and include files) as well as the new, revised, restructured or obsolete cal-G files refer to the respective Software Release notes and the analysis sections of the individual SCREWs and SPRs. For completeness, the following SCREWs and SPRs have been closed up to the current version of OLP (version 10b9)

2.1 SCREWs on CAM's OLP

2.1.1 Implemented SCREWs on SPC

SCREW271, SCREW301, and SCREW350.

2.1.2 Implemented SCREWs on AAC

SCREW213, SCREW231, SCREW280, SCREW301, SCREW329, SCREW331, SCREW335, SCREW342, SCREW360, SCREW364, and SCREW431.

2.2 SPRs on CAM's OLP

2.2.1 Implemented SPRs on SPC

SPR0125, SPR0278, SPR0284, SPR0900, SPR0957, SPR1111, SPR1162, SPR1196, SPR1228, SPR1238, SPR1241, SPR1258, SPR1267, SPR1305, SPR1311, SPR1324, SPR1328, SPR1540, SPR1547, SPR1557, SPR2018, SPR2081, SPR2174, SPR2190, SPR2294, SPR2367, SPR2371, SPR2509, SPR2638, SPR2660, SPR2784, SPR2789, SPR2840, SPR3003, SPR3062, SPR3276, SPR3300, SPR3352, SPR3375

2.2.2 Implemented SPRs on AAC

SPR0830, SPR0883, SPR0899, SPR0900, SPR1111, SPR1120, SPR1138, SPR1139, SPR1140, SPR1181, SPR1186, SPR1188, SPR1190, SPR1210, SPR1211, SPR1229, SPR1234, SPR1240, SPR1258, SPR1270, SPR1275, SPR1278, SPR1285, SPR1302, SPR1304, SPR1307, SPR1308, SPR1313, SPR1336, SPR1338, SPR1342, SPR1346, SPR1348, SPR1360, SPR1366, SPR1372, SPR1377, SPR1378, SPR1380, SPR1381, SPR1402, SPR1415, SPR1467, SPR1468, SPR1469, SPR1470, SPR1471, SPR1473, SPR1474, SPR1475, SPR1480, SPR1481, SPR1500, SPR1507, SPR1565, SPR1569, SPR1589, SPR1603, SPR1612, SPR1618, SPR1619, SPR1620, SPR1622, SPR1625, SPR1662, SPR1714, SPR1719, SPR1721, SPR1734, SPR1738, SPR1740, SPR1741, SPR1750, SPR1753, SPR1754, SPR1759, SPR1762, SPR1764, SPR1776, SPR1789, SPR1809, SPR1810, SPR1817, SPR1819, SPR1827, SPR1842, SPR1850, SPR1854, SPR1892, SPR1894, SPR1939, SPR1953, SPR1954, SPR1958, SPR1966, SPR1968, SPR1971, SPR1979, SPR1983, SPR2001, SPR2009, SPR2017, SPR2028, SPR2039, SPR2048, SPR2060, SPR2061, SPR2090, SPR2126, SPR2134, SPR2151, SPR2170, SPR2171, SPR2192, SPR2202, SPR2208, SPR2211, SPR2213, SPR2218, SPR2221, SPR2222, SPR2223, SPR2229, SPR2231, SPR2232, SPR2233, SPR2235, SPR2243, SPR2254, SPR2285, SPR2303, SPR2304, SPR2308, SPR2309, SPR2318, SPR2320, SPR2340, SPR2349, SPR2351, SPR2370, SPR2374, SPR2382, SPR2400, SPR2403, SPR2457, SPR2491, SPR2547, SPR2548, SPR2550, SPR2565, SPR2568, SPR2574, SPR2576, SPR2577, SPR2578, SPR2581, SPR2583, SPR2585, SPR2606, SPR2611, SPR2615, SPR2617, SPR2638, SPR2639, SPR2640, SPR2687, SPR2690, SPR2717, SPR2782, SPR2787, SPR2817, SPR2849, SPR2873, SPR2881, SPR2883, SPR2886, SPR3080, SPR3203, SPR3223, SPR3225, SPR3247, SPR3257, SPR3261, SPR3262, SPR3263, SPR3272, SPR3277, SPR3279, SPR3285, SPR3287, SPR3288, SPR3289, SPR3298, SPR3318, SPR3333, SPR3350, SPR3353, SPR3358, SPR3410, SPR3421, SPR3423, SPR3426, SPR3442, SPR3495, SPR3516, SPR3553, SPR3602, SPR3615, SPR3616, SPR3620, SPR3621

3 Comments on some major implemented SCREWs/SPRs

3.1 Improved CSTA and CISP generation

Major SPRs involved: 2580, 3369. Fig 2 shows the histogram of the ratio of CISP to CIER records. As expected there are two major peaks: when CAM is in the on–board processing, there should be as many CISP as CIER records; this is the peak at ratio unity. In normal processing mode there should be one CISP record per two CIER records; this is the peak at ratio one/half. Note that there is very little dispersion around the two canonical values.

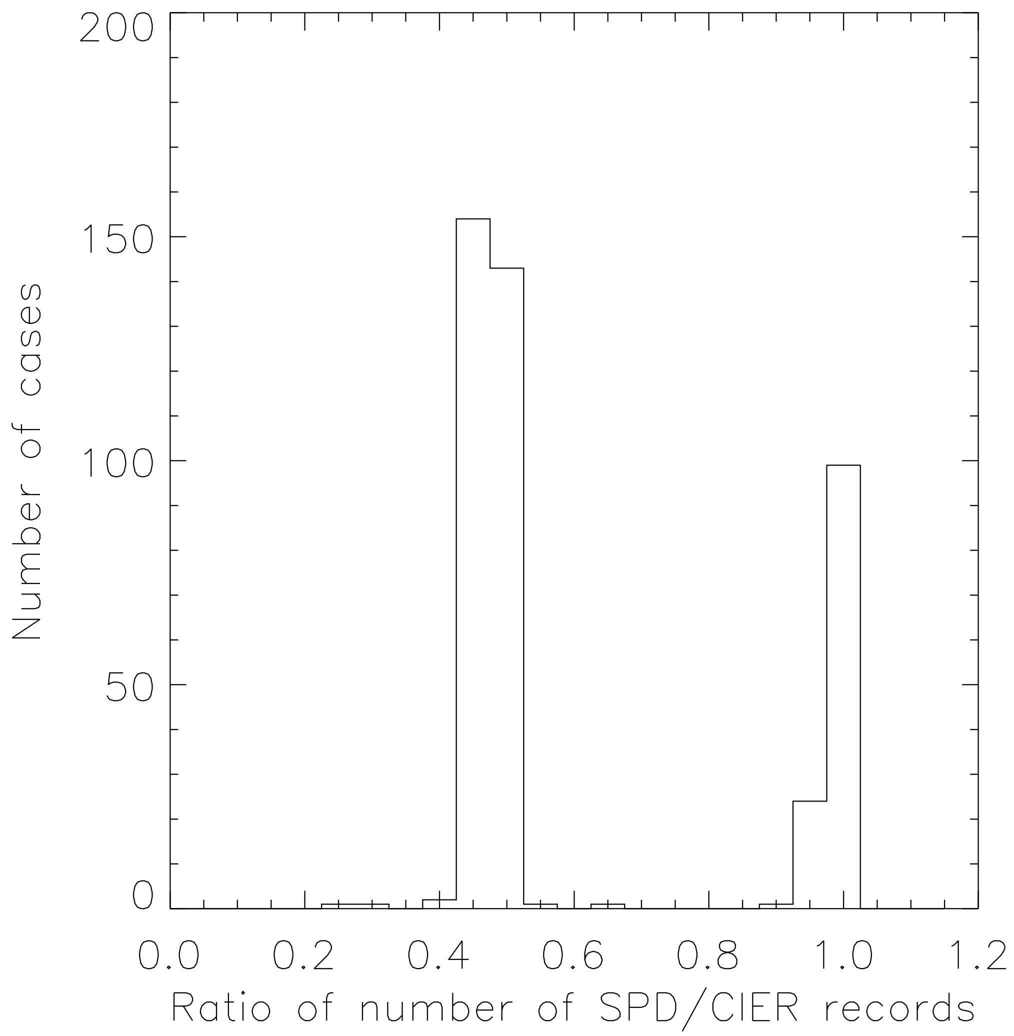

Figure 2: Histogram of the ratio CISP to CIER number of records

3.2 LW detector transient corrections

The algorithm introduced in OLP is the same as used by CIA and therefore has the same shortcomings: point–like sources are not correctly handled. However, there is no negative impact on point sources, see Section 7.

As an example, Fig 3 shows the spectrum of IC443 as obtained from olp10 with correction and as obtained form CIA without correction. The CIA corrected spectrum (not shown) is very close to the OLP corrected spectrum.

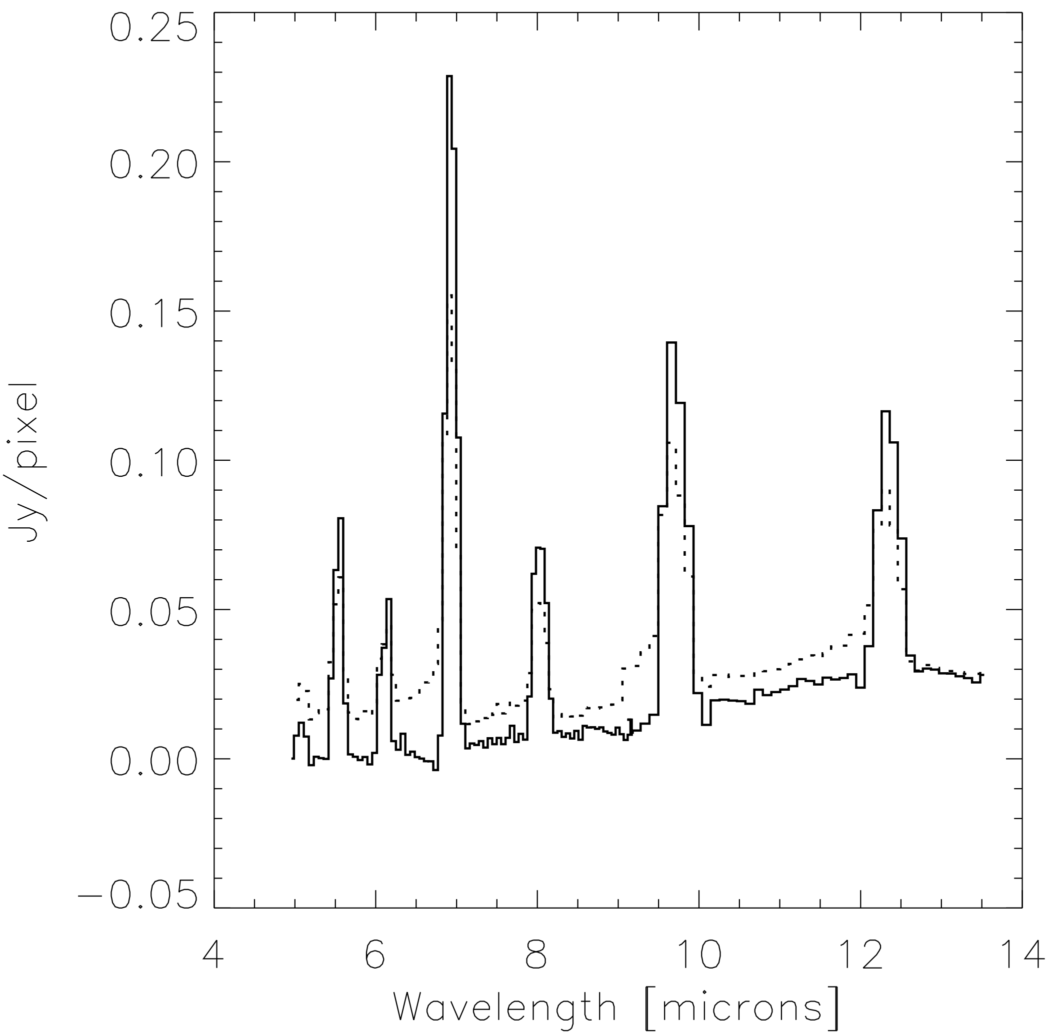

Figure 3: Spectrum of IC443 with transient correction (solid) and without (dotted). The peak strengths are noticeably stronger and the line bases are narrower. Notice also that the baseline at short wavelengths has become much closer to the no emission level.

Figure 4 shows another example of the improvements introduced in olp10b9 by the transient corrector. A reconstructed raster map of M51 is presented (taken from OLP's CMOS product file). The left image is that of olp10b9; the right one comes from olp9.1. Both images are copied using exactly the same set of up and low cuts (0.005 and 0.003 respectively). The first most evident difference is the almost total removal of the ghost image of the bright companion, the leftmost bright object in the images. The second obvious difference is the elimination of the fuzziness between the spiral arms, due to remanence effects. The third obvious difference is the enhanced arm – interarm contrast visible in the olp10b9 image.

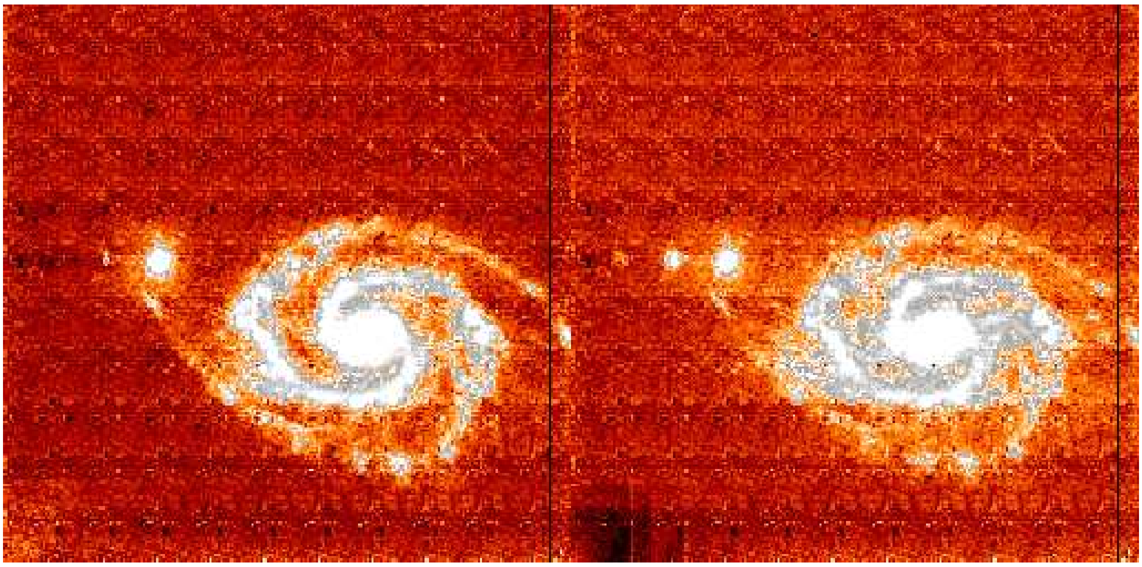

Figure 4: Image of M51 with transient correction (olp10b9, left) and without (olp9.1, right). Remark that most ghost images have almost disappeared, particularly the ghost of the strong companion to M51

3.3 New Point Source Detection algorithm

Two SPRs deal with this problem: SPR3271 and SPR3553.

Find below the analysis and the solution of SPR3271 implemented in the current OLP.

```
Number:                3271
Title:                 AACs point source determination
Originator:            so
Date:                  20000410
Affected SW:           OLP(CAM)
Version:               8.0.b.3
Priority:              NORMAL
Environment:           std
-----------------------------------------------------------------
Problem Description:

AAC finds too many pointsources, even in the airy ring of point source
measurements. To get rid of this caveat, AACs point source determination
has to be brushed up in olp10.
-----------------------------------------------------------------
Analyst:               APO
Analysis Date:         20000410
Problem Analysis:
        AAC detects point sources by PSF fitting but only does a single
source
        in a detection cell whose size is determined by the extent of
        the relevant PSF and which is always much smaller than the 32*32
        image.
        The Airey rings fall outside the detection cell and thus trick AAC
        into spuriously identifying them as other sources. The improvement to
        be made is simply to be able simultaneously to model two or more
        sources or as many as required over the whole field of view. The
```

```
        single source algorithm is simple and fast because there is an
        analytical solution.
        A multiple source replacement would involve the solution of a more
        complex set of linear equations - or better becuase I know how to
        do it - iteration in multidimensional parameter space.
Recommended Solution:
        Introduce multiple simultaneous sources into AAC's source detection
        method as modified by SPR3553.
```

Next find the analysis and the solution of SPR3553 as now implemented in the current OLP.

```
Analyst:                APO
Analysis Date:          20010214
Problem Analysis:
        This is a problem that should have been tackled years ago. It arises
        from a combination of AAC's literal interpretation of the Flux errors
        given in the CMAP images combined with the Gaussian PSF fitting method
        employed. The best-fit intensities of source and background involve
        summations over the 32*32 pixel array of terms such as Sum(w*p*f),
        where the weight w=1/df^df, f=Flux, df=Flux error and p=psf value, and
        for large Flux errors, this weights the brightest pixels less than you
        might expect. The equivalent CIA routine ignore the errors. The
        quadratic nature of the chisq statistic also has the curious
        consequence that the final minimum chisq model, m, satisfies a
        non-linear condition Sum(m*m) = Sum(d*d), rather than the more
        intuitive linear condition Sum(m) = Sum(d) which is also implicit in
        aperture photometry. There are therefore two separate though connected
        threads to follow.
Recommended Solution:
        I've often used Poisson statistics before to do this type of job. They
        have the advantage that the final model satisfies the intuitive linear
        condition. The data are not Poisson in nature, so there remains the
        need to devise an so-called equivalent Poisson map which will preserve
        or perhaps reproduce or perhaps simulate an image's noise amplitude.
        There are two approaches one could adopt based on either the CMAP error
        themselves or on the observed spread of the Flux values. These two
        estimates should give the same answer. Experience shows that they
        don't and that sometimes one is better, sometimes the other. Therefore,
        an empirical approach should be adopted and choose whichever estimate
        is the more conservative. If the noise is too small, you get lots of
        spurious sources - and this has probably accounts for some of AAC's
        trouble in the past with too many sources; if the noise is too big you
        needlessly throw away perfectly good sources. There is also a need to
        introduce quality measures to ignore the relatively high proportion
        of transient-corrected Fluxes that appear negative in the CMAP files
        and to screen out spurious sources clearly caused by edge effects. A
        good deal of reorganisation is required and much of the work is in
        common with SPR3271, to which reference should be made.
```

The above SPRs were introduced to solve two problems: (1) under–evaluation of Fluxes, and (2) detection of "bogus" point–like sources. For the success of (1) please see section 7; for the success of (2) note the following. The previous version of OLP would report a grand total of 51941 point sources amongst the 424 test cases; the current version reports only 12582 point sources, only 25% of the previous total.

Careful screening of several test cases shows that indeed "bogus" sources are no longer detected but it was also noted that some "real" looking point sources escape detection. We think that altogether this is

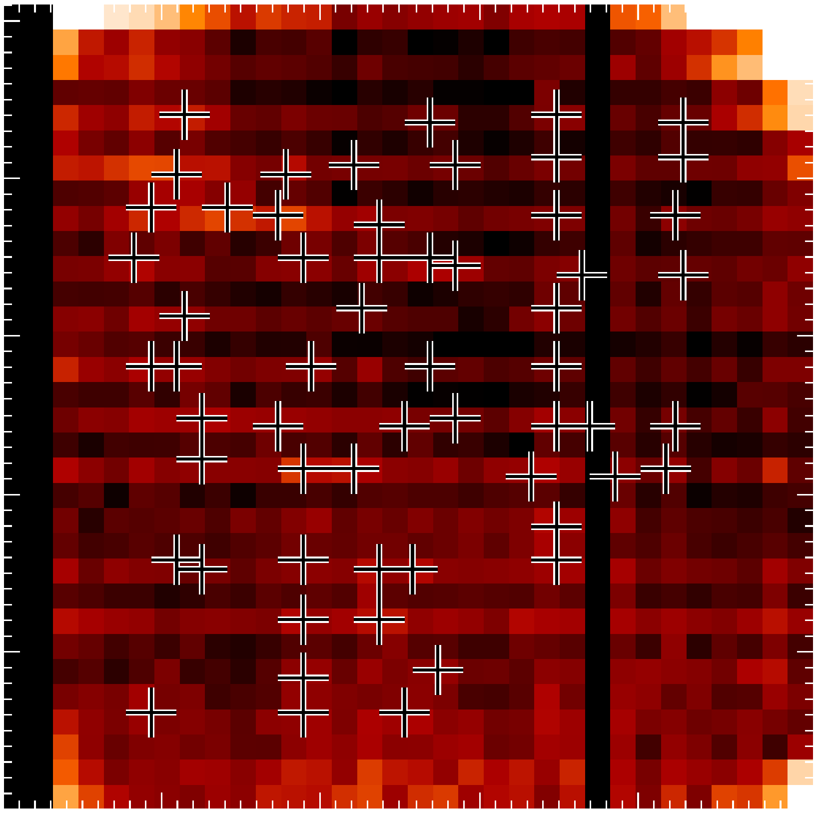

Figure 5: “Bogus” point–like sources found by previous OLP (shown as crosses on a CMAP plane from TDT 57200101)

a preferable situation as to that of dozens of non–existing sources being claimed as real. More on this in section 8.3.4.

An extreme example of the improved algorithm is illustrated by Figures 5 and 6, representing the first CMAP image for TDT 57200101. Where previous versions of OLP would find more than 50 questionnable sources, the current version finds none, as it should be the case, Fig. 6.

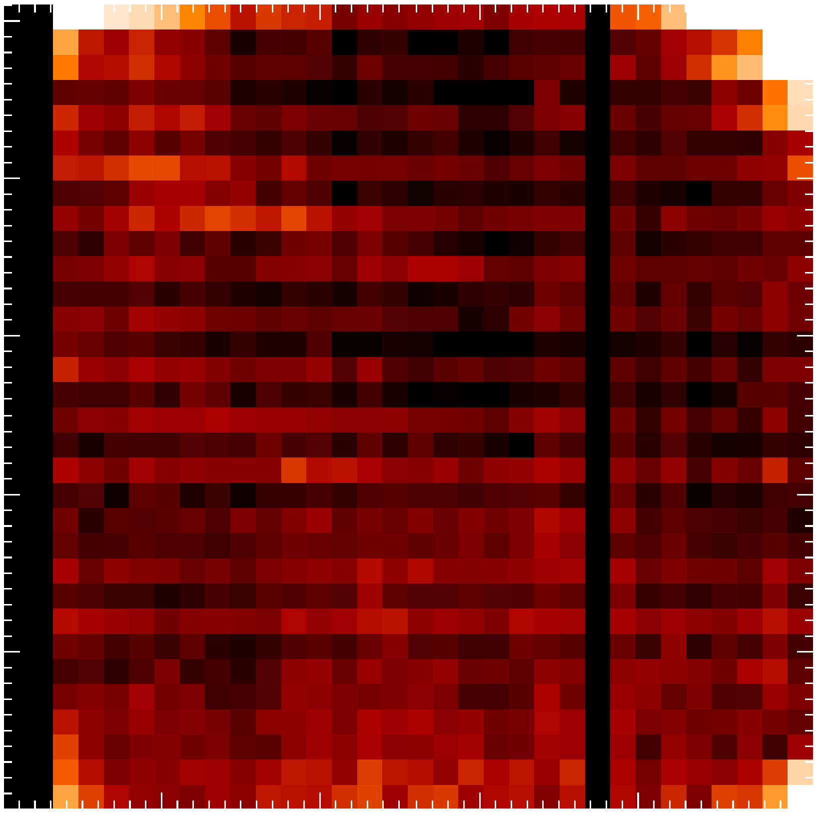

Figure 6: Same field as Fig. 5. No point–like sources are found by the current OLP

4 SPRs and SCREWs not closed for the "Legacy Archive" OLP

Several SPRs and SCREWs could not be closed on time for the delivery deadline of the legacy OLP, see Tables 2 and 3. With one or two exceptions, noted below in the "NOTES" sections, none of them affect any large number of CAM's observations. In fact, many of them refer to non AOT driven observations.

4.1 Open SPRs

4.1.1 Notes to Table 2

Still open SPRs are shown in Table 2 above. Their title, as recorded in the SPR database at Villafranca, is given in the Table. For further information, the full text from the Software Problem Report (text in italics) has been reproduced *verbatim.*

SPR2375 *The mosaics of what appears to be all the observations in the GSPEAR GS_BM_1 programme are of poor quality. In particular, they exhibit a "wire mesh" effect with a Flux variation in both dimensions with 2-pixel frequency. This effect may well be related to SPR 2303 - Return of the Disjointed Mosaic.* And the analysis says:

I've spent days looking into this one - with no definite conclusion I'm sorry to say. The mosaics are indeed covered in interlocking linear features but which are nothing to do with the disjointed mosaics of SPR2303 and other SPRs. The observation was a micro-scan with a 2-pixel raster step size - hence the spatial frequency Steve mentions above - in which there is a one-to-one correspondence between CMAP and CMOS pixels and thus no coverage problems of the disjointed mosaic type. I've also tried in vain to find similar effects in other observations taken in the same instrumental configuration. One important piece of information from Steve is that CIA, which uses a completely

Table 2: Open SPRs for OLP version 10

SPR	Title
SPR2375	AAC - The Wire Mesh
SPR2396	Illumination mask should not blind CMAP
SPR2413	AAC's treatment of off-target images
SPR2586	Non synchronziation related subscript 1 range error?
SPR2654	CMOS in the CUFF — as times go by
SPR2659	Proper closure of CUFF
SPR2781	Happy christmas derive SPD
SPR2790	D-SPD for CAM : from parallel to prime into the nowhere
SPR2798	CAM parallel recovery from worst-case CCS on hold
SPR2811	CAM AAC illumination masking ... the story continues
SPR2837	Apage idle states!
SPR2860	Illumination masking — the void holds no information
SPR2864	No CSSP entry for a detection at one wavelength
SPR2867	Quality measures to supress ugly CMAPs
SPR2880	A high performance trap caught CAM —— SPC
SPR2882	Fine-tuning the SPC IDLE mode starting logic
SPR2943	No polarizor information in C99s
SPR2966	Making good for CAM's missing CSH-discrepancy sum flag
SPR2992	Review of AACs reaction in case it encounters no useful data
SPR3100	The CAM pipeline speaks with a forked tongue
SPR3127	Different weights for aac's polarisation treatment
SPR3229	Discontinue all AAC's use of the EOHA
SPR3255	AAC and IDLE mode
SPR3297	Overruling the OTF flag during activation
SPR3308	Agony of aspect solutions
SPR3321	AAC's unhappiness with target not acquired
SPR3326	AAC performing miracles
SPR3355	Give cstacvfi a proper filling
SPR3359	Turning the CVF wheels too much
SPR3379	Remaining improvements for cam compact status
SPR3425	olp9 bored with 77701420
SPR3431	Strips (but no stars) in the CMAP error
SPR3448	Avoiding unnecessary file creation
SPR3495	CAM CAL-G files for OLP v10
SPR3528	The wavelength of AAC's CMOS 01402705
SPR3597	Misspelling of schubert
SPR3607	CSTA incomplete for 195 005 13
SPR3608	AAC misses nice last image for for 195 005 13
SPR3612	Saturations remain undetected by AAC
SPR3655	CAM compact status – the saga continues
SPR3664	C62 and C63 processing failure reopened
SPR3665	A special case of SPR3664
SPR3666	Processing failure for TDT 586984001
SPR3667	First SPR related to CAM processing failures
SPR3668	Second SPR related to Screw 423
SPR3669	Third SPR related to Screw 423

different mosaic algorithm, finds the same trouble. My own suspicion is that the stripes reflect low-level systematic errors in the CAL-G files but I'm a few days work or more away from proving that. There's nothing wrong with OLP as far as I can tell.

The "wire mesh" affects only CMOS–like products. Very likely it arises from a poor flat–field correction whereby the overlapping (or contigous) areas of a raster scan becomes visible to the eye.

SPR2396 *The current implementation of the illumination mask sets the affected pixels of the CMAP to undefined. While the effects of the illumination masking are very beneficial for the (non) detection of spurious point sources and for the final mosaic, the user looses valuable information about the lens wheel jitter (which is also beneficial for the quality check point of view). Therefore the illumination masking should not affect the view of the CMAP, but only the higher processing steps.* Its non implementation has no consequence whatsoever on the accuracy of the data products.

SPR2413 *There are occasions when the AOCS system fails to find the guide star and announces via the APH that the target has not been acquired, in which case AAC is confined to calculating the products like CCIM and CGLL, which relate to how the detectors performed. The CMAPs that contain images of the sky, and the other products derived from them, are not made. There are often cases where this restriction is unnecessary in which, the pointing is apparently stable enough but, perhaps, 20" from where it should be. Recently, for example, on behalf of Lex Kaper, I tricked AAC into ignoring its usual logic for the Vela X-1 observations (190002,61), (190002,05) & (190002,62) that the APH showed were off-target and derived some beautiful images that were just what the Dr Kaper had ordered. We should consider doing this type of thing on a routine basis for OLP v7.* Its non implementation has no consequence whatsoever on the accuracy of the data products. The very few cases of pointing errors have no CMAP/CMOS products in the archive.

SPR2586 *non synchronziation related subscript 1 range error?.* Its non implementation has no consequence whatsoever on the accuracy of the data products as there are no products generated when this error condition is encountered.

SPR2654 *The exposure time of the CMOS in the CUFF is wrong.* TBW

SPR2659 *After AAC issues its famous message*

```
AAC v7.0.13 starting at 13:02:49 on 1-JUN-98
CCD v4.4 calibration data release
Aspect solution not found : SPD out of synchronisation with the IRPH
RPID=[1,1] 238542476.4583333<UTC<238542501.6666666
```

it quits. This information is kept in the cuff.dat file. However, NAXIS2 remains set to 0, with the consequence that the corresponding *.fits file is empty — which is a pity, because this is the one being archived. An example is 25000152.* The SPR may have been serendipitous fixed with some other SPR as the problem no longer appears.

SPR2781 The problem is a non nominal datum range in the raw telemetry which causes the decoding algorithm to issue a warning. Has no impact on the accuracy of the data products.

SPR2790 It describes a failure of the Standard Product Derivation pipeline step. In this case no data products are generated hence none of the archived products have suffered from this condition.

SPR2798 *S01(135018,27) and S06(491011,14) are two examples of observations which fail post SCREW300 during DERIVE_ERD generation of the CAM parallel pointing files because the CCS was on hold when the telescope was supposed to move to the following target and begin a new observation. The new observations' EOHA, EOHC and APPH entries are all missing. Both these example missing observations were rasters which strangely enough appear to have survived to the extent that an unexpected change from RPID=[1,1] to [2,1] is what causes DERIVE_IPH to give up. There are probably other raster and non-raster examples to be found using more sophistocated procedures than those used to produce the list of outstanding pointing problems provided to the CCB, which was based on the contents of the set of APPH and EOHA files..* Whatever the cause of the problem, it does not affect archived data products.

SPR2811 *While SPR 2351 improved the illumination masking, it is still not ok: The observations 55501033, 70900102, 70900134 and 70900204 were failed due to a bad illumination masking of Auto Analysis.* The problem evoked here is an alleged failure of the pipeline code to recognize non–illuminated detector rows and/or columns. The problem does not affect the inner pixels and has no consequence on the detection and photometry of point sources (the product CPSL).

SPR2837 *It has transpired that the IDLE mode in ISOCAM was originally introduced to provide a time-buffer until the instrument and the satellite reached their observing condition. However, with the a reliable CSH discrepancy flag and a on-target flag available, this condition can be over-ruled and one gains additional readouts.* No consequence whatsoever on archived products as SPD now overules this flag.

SPR2860 *Obs 01401716 is a SW observation with the small mirror. AAC tries to guess the un-illuminated parts of the detector ... but, in the absence of any background, it has to guess blindly and therefore badly. Therefore AAC's illumination masking should be reviewed, and no masking performed in the absence of a clear background.* Be cautious of outermost rows and columns when using SW detector archived products.

SPR2864 *No CSSP entry for a detection at one wavelength.* Irrelevant to the archived data products

SPR2867 *After the introduction of SCREW 300, AAC gets more data to handle, including very short SCDs stemming from a transient state. While it is a proof of AAC's robustness that it handles also these data (which are often only one or two readouts), the resulting CMAPs look ugly and give a wrong impression of the CAM products. An example is 03803505 — the first CMAP displayed is actually only one readout, with its middle masked. Instead, there should be a minimum number of readouts to create a CMAP. This minimum number might have to be flexible to handle lunatic observations where the state changes very rapidly(fast rasters, fast polarizing observations like 03804901 and 03805001 and the CVF speed trip 30201662, who has sometimes only one readout with a good CSH discrepany flag).* Beware of CMAPs made from a few detector readouts (see corresponding CUFF).

SPR2880 *D-SPD crashed for observation 46980500 via a high performance trap in the routine UTK_UTC0.* Failure of Standard Product Derivation for one observation. Since no products are produced, the SPR does not affect the archived data.

SPR2882 *SPR 2840 nearly solved the problem of SPC IDLE mode starting logic. One observation, 65580100, however, defies even the last attempts: f2aotopm in cper65580100.fits 001111; cpspobst in cpsp65580100.fits 001111.* No impact on archived products.

SPR2943 *For 82201602, which is a raster with polarizor 1, there is no indication in the CUFF that the observation was done with a polarizor.* The CUFF product for some CAM99 observations may lack the polariser information.

SPR2966 *In observation 34901528 (CAM parallel) the entrance wheels moves from 6" (360) to 1.5" (192) and the filter wheel from LW4 (305) to LW3 (125) between record 1 to record 2. With the wheel parameters downlinked at the end of one image, this means that during record 2 the wheels changed, and the data taken during this period should be ignored. However, SPD's discrepany flag remains at 0 (good) — I assume because it is computed by comparing commanded and actual wheel positions, which are ok at the time of sending down the CAM —— frame.* Too time consuming to solve given the negligible incidence on archived data products.

SPR2992 *Understanding that the decision of the archive scientist for SPR 2952 will be not to distribute OFRP products if they failed at this processing level, AACs reaction in case it encounters no useful data should be changed from a abnormal termination (via MCQUIT) to a QC Level 1 message.* No incidence on archived data products.

SPR3100 *SPC uses the (unmaintained) CWHEELS file to get wavelength and bandwidth for fixed filters. THis results in a discrepancy, e.g. for LW3 SPC reports a wavelength of 14.5 while AAC (as stated in the CAM handbook) gives 14.3. The same is true for the bandwidth: 3 micron for SPD, 5.5 micron* *for AAC. To avoid a baffling of users, SPC should either use the SPEC instead of the CWHEELS file and the caveats should be updated to reflect that the CWHEELS file contains outdated values or the CWHEELS file should be updated and its maintainence of the CWHEELS should be linked to the SPEC file.* This fact will be included in the caveats to SPD (see 8.2.1) .

SPR3127 *In the moment aac reads the polar weight factors from the ccglwspec file. however, while the sensitivity is independent of the lens (see Blommaert et all), the polar weight factors are different for different lenses (see the article of Siebenmorgen). AAC has to get the information from a different source or the information in the ccglwspec file will have to be replicated.* Real impact on data products not yet evaluated.

SPR3229 *SPR3203 was concerned with AAC's use of the EOHA to calculate something it needs for its CAL-G files. There are other places in which EOHA data are used, including EOHA keywords which have been transfered to SPD headers. Where possible these should be replaced by the corresponding EOHC quantities as CAM's OLP has to work when there is no EOHA entry. Those EOHA keywords might be interesting.* Believed to have no incidence on archived data products.

SPR3255 *SPR2881, SPR2883 and SPR2787, among others, focussed attention on AAC's treatment of IDLE-mode records in SPD. There is even the suggestion in SPR2837 that all IDLE modes should be overruled. Following SPR1759 (ancient history), AAC sometimes makes up IDLE modes of its own that has the effect, for example, of sabotaging the fix for SPR2881 by overuling all the dark measurements of 25102703 for supposed reasons of consistency. AAC's use of IDLE mode in this way should be thoroughly reviewed. Other TDT affected, discovered by SO on 03/08/2000 66801791.* Real impact on data products not yet evaluated.

SPR3297 *SPR3296 described a potential problem with d_iph. If it is confirmed, also the OTF Flag in CAM ERD and SPD has to be overruled during activation (and, possibly, during deactivation).* No incidence on science archived data products.

SPR3308 *During the pointing validation exercise 327 observations which crashed beforehand at D-IPH level were processed until AAC. 21 observations crashed with aspect solution not found. With IDA/OFPR down, a slighly arkward processing route had to be choosen: get aocs, cper, csta, apph, eoha + eohc from OLP7 IDA, rederive pointing files with D-IPH v9 (APo master version), create SPD files with SPC v90b5, create AAC files with AAC v90b5. The problem cases are....* No incidence on archived data products.

SPR3321 *In observation 60200101 the target is not acquired at all. First, this leads to n aspect solution not found error — is it necessary to try to find the aspect solution if the target is not acquired? Finally, AAC crashes.* No incidence on archived data products.

SPR3326 *In the CAM —— image 86592300 AAC creates one (and only one) 31*32 CMAP. However, the resulting CMOS is 32*33 big. One might want to review the mosaic generating algorithms to stop this replication.* Breadth of the problem not known but likely to be very narrow as none of the hundreds of validation TTDs show this problem.

SPR3355 *While looking for means to select upward/downward scans, John told me that cstacfi contains only the values 0, 1 or 2.*

0 (example is 05804802) is invalid for a CVF scan. Also I remember observations with a CVF increment of 4. (note that this problem might have been fixed by implementation of SPR 3284)

However, for 10402702 cstacfi has the value 1 despite the fact it is an upward and downward scan, where 1 and -1 would be more suited as they also indicate the direction. No incidence on archived data products.

SPR3359 *Observation 05805509 overshoots the calibrated CVF range by far. Instead of stopping at step 235, it goes to 241. While AAC properly does not convert the CCIMs into CMAPs, the reason for this is somewhat hidden from the user: CUFF reports only : inconsistent optical configuration (which is not really applicable in this case) If it is a small effort, maybe one can give a better warning.* No incidence on archived data products.

SPR3379 *Skimming through the latest CSTA files of the official testcases, several empty CSTA's have been found, despite that CIA reports there are at least 4 readouts with the same camera configuration the SPD files.* No incidence on archived data products.

SPR3425 *77701420 is a rather boring observation, containing in OLP 7 no CMAPs (but 9 CCIMs). However, CAM OLP9 took offense and decided not to produce any product (and crash?). It should be reviewed whether the production of CCIMs can be revived.* No incidence on archived data products.

SPR3431 *Following up on SPR 3426 I noticed a strip pattern in the error part of the cmap file for the observations 12701113. As for this observation the CMAPs looks fine, there might be another error lurking in the dark. Also for 05000203 and 05001601 the CMAP error shows a dark pattern, however for these observations it is unclear whether also the CMAP is affected by SPR 3426.* No incidence on archived data products.

SPR3448 *In the hope of exciting pointsouces and spectra, AAC stars to open CPSL and CSSP files. However, if no entries are found, they should not be written to disk as empty fits files.* No incidence on archived data products.

SPR3495 *For OLP v10, an expanded and revised set of CAM CAL-G files is to be delivered. For example, the implementation of SCREW361 requires some extra sensitivity error values. Care should also be taken to include a proper CALIBRAT keyword header record, including the accompanying comment. The current set is rather heterogeneous.*

SPR3528 *The observation 01402705 implicated in SPR3514 is a 6*6 raster at 8.3-10.9 micron. Right at the beginning of the observation is what looks like the remnant of a preceding CAM parallel configuration at longer wavelength. One CMOS gets produced by AAC with the wrong wavelength. Here's the CUFF's version of events....* As far as it is known, there is no incidence on archived data products.

SPR3597 *AAC writes:*

FS:Using transient corrector Fouks-Shubert v2.0

this is misspelled and should be

FS:Using transient corrector Fouks-Schubert v2.0

This is the most important SPR that unfortunate could not be fixed given the complexity of the problem. Fortunately, it spares CAM parallel observations and all SW observations as it affects only CAM prime LW detector observations.

SPR3607 *csta appears to be incomplete for 195 005 13. there are 12 readouts in CAM —— configuration at the end, which don't make it into csta. also the timing of the last record is strange: why does a configuration of 2 2sec readouts last 27 sec?.* No incidence on archived data products.

SPR3608 *aac misses nice last image (12 cam —— readouts) for for 195 005 13. the quality flags are ok, mode is obs — and actually this image is better than the prime image, as it is not saturated....* No incidence on archived data products.

SPR3612 *Oobservation 19500513 shows strong saturation (ADC and quite likely also detector saturation). Regrettably, AAC does not notice it.*As far as we can see there is no incidence on other archived data products.

SPR3655 *Out of interest, the observation 84201714 was run under OLP 10b12. Sadly, d-erd did not create a record for 7 nice CAM parallel readouts.* May cause the non production of CSTA files in some other rare cases.

SPR3664 *SPR 3560 was raised during the Bulk reprocessing with OLP9.1 in several (if not all) C62 and C63 observations. That SPR was closed 20 days ago because the observations were successfully processed during a test with OLPv10b9 installed in Pipepar. However, now the OFRP with OLPv10 fails again with the same error message shown in SPR 3560.* No incidence on science archived data products.

SPR3665 *Although the failure of TDTs C62 and C63 are covered by SPR 3664, this is an special case among them since the SPC step is successfully completed but the failure is in AAC:* No incidence on science archived data products.

SPR3666 *The failure of this CAM // TDT was covered before by SPR2962 (related to the duplication of entries in the EOHC). However the new failure doesn't seem to be related to that SPR.* No incidence on archived data products.

SPR3667 *TDT 87200636 (C01) was the subject of SPR2813 which were closed with reference to Screw 423 for this observation. However when processing with OLPv10 the AA fails again.* No incidence on archived data products.

SPR3668 *As TDT 87200636 in SPR 3667, observation 135018271 (C //) was apparently covered by SCREW 423. However the AA fails with OLPv10.* No incidence on archived data products.

SPR3669 *In this case the affected TDT is 77701919 (C01) for which the error message displayed by the AAC journal file is....* No incidence on archived data products.

SPR3695 *During the BKRP with OLPv10 three CAM observations failed in AA with a new error. The affected TDTs are: 16300201, 44900303 and 49400988.* These observations will not be in the archive.

SPR3696 *Four C99 observations failed during the BKRP with OLPv10 with the same stack dump reported in the old SPR 2687 (OLPv7.01).* These observations will not appear in the archive

4.2 Open SCREWs

Table 3: Open SCREWs for OLP version 10

SCREW	Title
SCREW301	Improvement of the CSTA generation and layout
SCREW361	Inclusion of sensitivity error for CAM products
SCREW363	Discrepancy flag for CAM ERD
SCREW371	Visibility of ISOCAM's illumination masking
SCREW417	Sky-flatfielding with AAC
SCREW427	OLP and CAL-G Encapsulation of the 0.7s AOCS delay

4.2.1 Notes to the open SCREWs

SCREW301 *In the moment the CSTA generation is triggered by the OPER_STEP key-word, set in the logic, and downlinked in CAM telemetry.*

Therefore, if this keyword is not set appropriately (e.g. in some COIFs) or in case of telemetry loss during an infavourable moment, then no CSTA will be generated. As a result of this, the product is not queryable in the CAM archive screen, which contains the CAM configuration and is the main resource to obtain suitable calibration data.

Also the CSTA generation for CVF scans is deficient: Instead of describing all CAM configurations performed during a CVF scan only the first setting is put into the CSTA. Therefore it is impossible to query products for specific CVF configurations.

The CSTA should be also amended to contain a more complete description of the instrument state (e.g. gain, on-board processing mode...)

The analysis of this SCREW concluded that indeed it implied three different changes to the CSTA generation algorithm:

1. Change the contents of CSTA

2. Create CSTA records for *each* CVF state
3. Change the logic to produce a CSTA record when the relevant telecommand signals are missing (some COIF observations) or have been lost due to a telemetry dropout.

Only changes 1 and 2 were actually performed. This means that in some very rare ocasions, the CSTA file may be missing some actual CAM configuration.

SCREW361 *Up to now, the error in the sensitivity factor is not given in the Cal-G files. After this uncertainty is available in the Cal-G files, AAC should be modifyied to take this into account.* Although the errors are now in the CAL-G files, AAC was not modified to read it and perform an error propagation calculation.

SCREW363 *It has lately transpired that F1 blocks, containing the cam instrument parameters, are generated independently from the F2 blocks which contain the detector dat Consequently this means that we are not sure about the cam instrument parameters if we look only at the f1 block succeeding (in time of generation) the f2 block. Instead, the parameters of the preceeding and the succeeding block have to be compared, and in case of a discrepancy (e.g. in case of a fast CVF scan), a discrepancy flag on CAM ERD level has to be set so that the data are ignored for image generation.* The impact of this - unlikely - situation is minimal compared to the modifications that should have been performed upon the computer code.

SCREW371 *AAC detects and masks out un-illuminated areas of the detector, an essential step to produce correct mosaics. However, it is also interesting to see how the (single) image looked before the masking — for the experienced user this can yield very useful information. SPR 2396 captures this information, but appends it (on a configuration per configuration base) to the CCIM file — which will only confuse normal users and is therefore considered a non-optimal solution.*

Instead, a new product (CILL?) should be created, which holds this information.. Although potentially useful for the experienced archive user, this SCREW was never implemented.

SCREW417 *one of the biggest pbs with AAC (apart from transients), is that it does not use sky-flat-fielding, but accesses the internal library flat-fields instead. Due to ISOCAM's wheel jitter, the resulting image can be very poor.*

With the implementation of screw 330 not to be expected before OLP10, the community could already benefit with OLP9 from this upgrade.

The only (minor) difficulty is how to give a criteria to apply sky- flatfielding — but using processing options this choice might be given to the user. The so called "minor" difficulty was impossible to overcome blindly, i.e. without human intervention, and hence not applicable to the automated pipeline.

SCREW427 *There is general agreement that there is a delay of unknown origin between science data and the accompanying AOCS data in telemetry. The best estimate of the delay should be made available to OLP and used wherever deemed necessary.* The ISOCAM team never found compelling evidence that indeed the so called 0.7 sec delay was applicable to CAM's data.

5 Photometric accuracy of calibration stars

The following Hypparcos Input Catalogue stars have been used throughout the ISO mission to calibrate ISOCAM: **HIC67485, HIC69713, HIC70218, HIC73005, HIC77277, HIC77760, HIC85317, HIC89474, HIC94376**, and **HIC94890**.

The following plots indicate for each star, and for *all* observations of that star, the Flux determined by OLP as a function of wavelength in case of multi–filter or CVF observations. The model Flux is overplotted to show the goodness between the measurements and the models used to derive the calibration curves. In many cases, the same star has been observed with various apertures, viz. 1.5, 3.0, and 6.0 arcsec per pixel; appropriate symbols indicate the apertures in the plots.

The plots have been generated automatically reading the CPSL (CAM Point Source List) file. The plots show:

- (Upper panel) Observed (several symbols according to PFOV) and HIC model Flux versus the wavelength
- (Middle panel) Measured DEC error versus RA error (with respect to HIC star nominal coordinates); same PFOV symbols.
- (Lower panel) Flux error versus wavelength; same PFOV symbols.

Some HIC observations have been performed in the raster mode. OLP does not find the Flux of sources in the resulting mosaic. Instead it finds Fluxes on the image produced for each raster leg. Take for instance the observations of HIC69713 (see below). Each was performed as a 4×4 raster and OLP searches for point objects in 16 different sky images. Hence there will be 16 brightest objects for each instance of a HIC69713 observation (one per raster position). Furthermore, this HIC star was observed 6 times during the mission. Hence, there are altogether 96 independent observations of the star. All 96 observations can be used to establish the repeatability of the Flux determination process; the repeatability is measured by the number following the Flux determination. This can also be seen in the plot corresponding to HIC69713, fig. 8, where a rather large dispersion of Fluxes measured at 4.5 microns can be seen; the dispersion amounts to 30 percent rms and the mean Flux is 35 percent lower than the model Flux.

5.1 HIC67485 - Plots and Tables

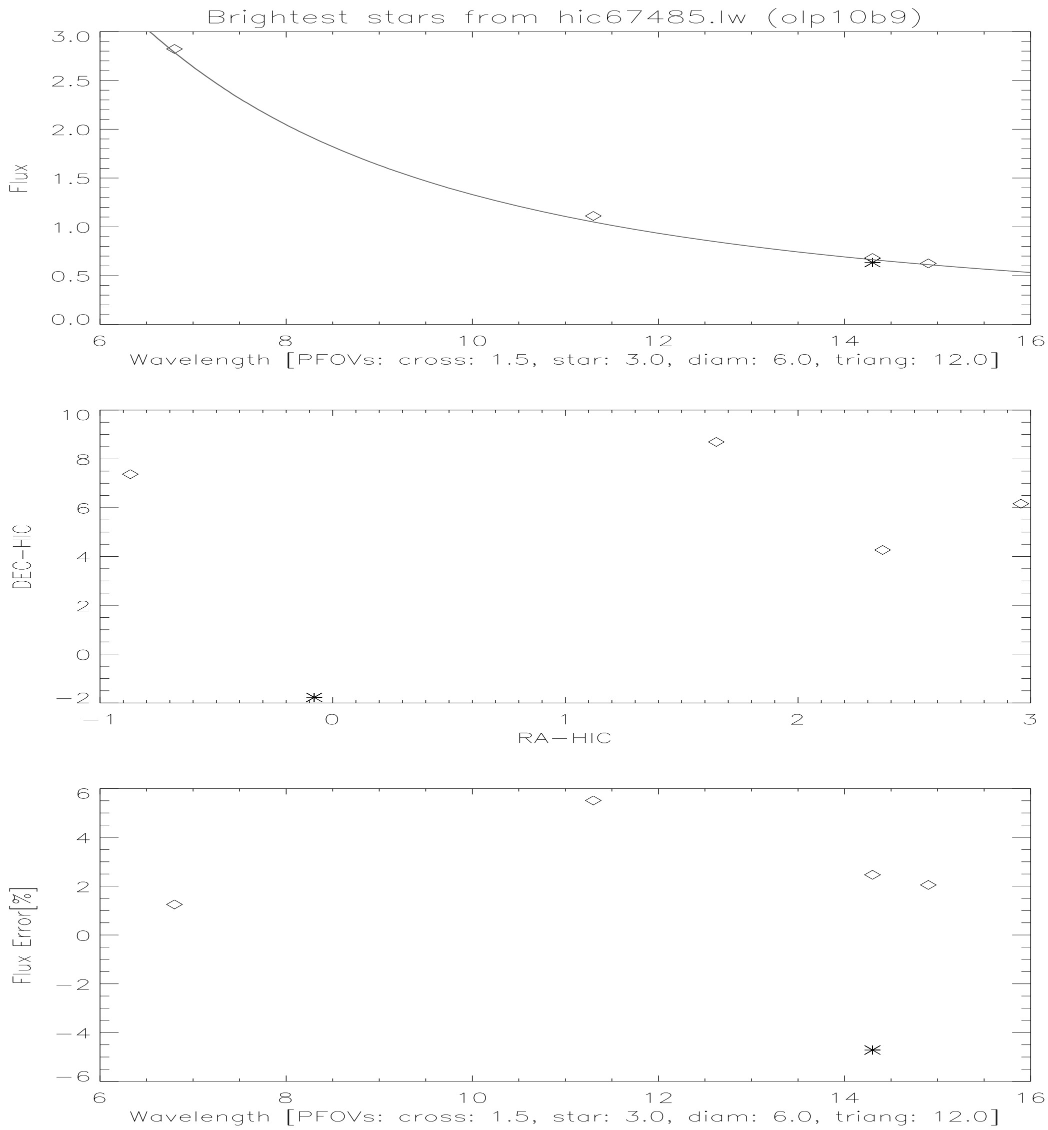

Figure 7: Plots for HIC67485 from olp10b9

TDT numbers of the observations used to create graphs and tables are: 41900718, 41900819, 41900920, 41901021, and 41901122.

The information displayed in the following Table, and all similar tables for the HIC calibrators is as follows:

- The number of times the given HIC star has been observed at the given wavelength. The number includes all Pixel Field of View observations
- The wavelength of the observations
- The (mean) Flux at the indicated wavelength
- When several observations have been made, the column indicates the RMS dispersion amongst observations, i.e. the repeatability of the measurement

- The difference between the model Flux and the measured Flux
- The TDT of the observation(s)
- The last entry gives the total number of times the HIC star was observed and the mean of the per wavelength error

The information following the table is

- The total number of observations of the HIC star
- The mean Flux error (all wavelengths and all PFOVs)
- The mean measured RA and DEC
- The nominal RA and DEC of the HIC object
- $Measured - Nominal$ RA and DEC, expressed in arcsec

```
Opening HIC67485.TAB
   1 stars   at 6.80E+00 mic; Flux: 2.82E+00       Error:   1% TDT: 41900920
   1 stars   at 1.13E+01 mic; Flux: 1.11E+00       Error:   5% TDT: 41900819
   2 stars   at 1.43E+01 mic; Flux: 6.57E-01+-  0% Error:   0% TDT: 41901021
   1 stars   at 1.49E+01 mic; Flux: 6.25E-01       Error:   2% TDT: 41900718
Grand total of    5 brights stars
Mean error all wavelengths:   2%

Mean : RA: 13h49m45.68s DEC:   61d29m26.5s
HIC  : RA: 13h49m45.51s DEC:   61d29m21.5s
DELTA: RA:  1.2 [arcsec];  DEC:  4.9 [arcsec]
```

5.2 HIC69713 - Plots and Tables

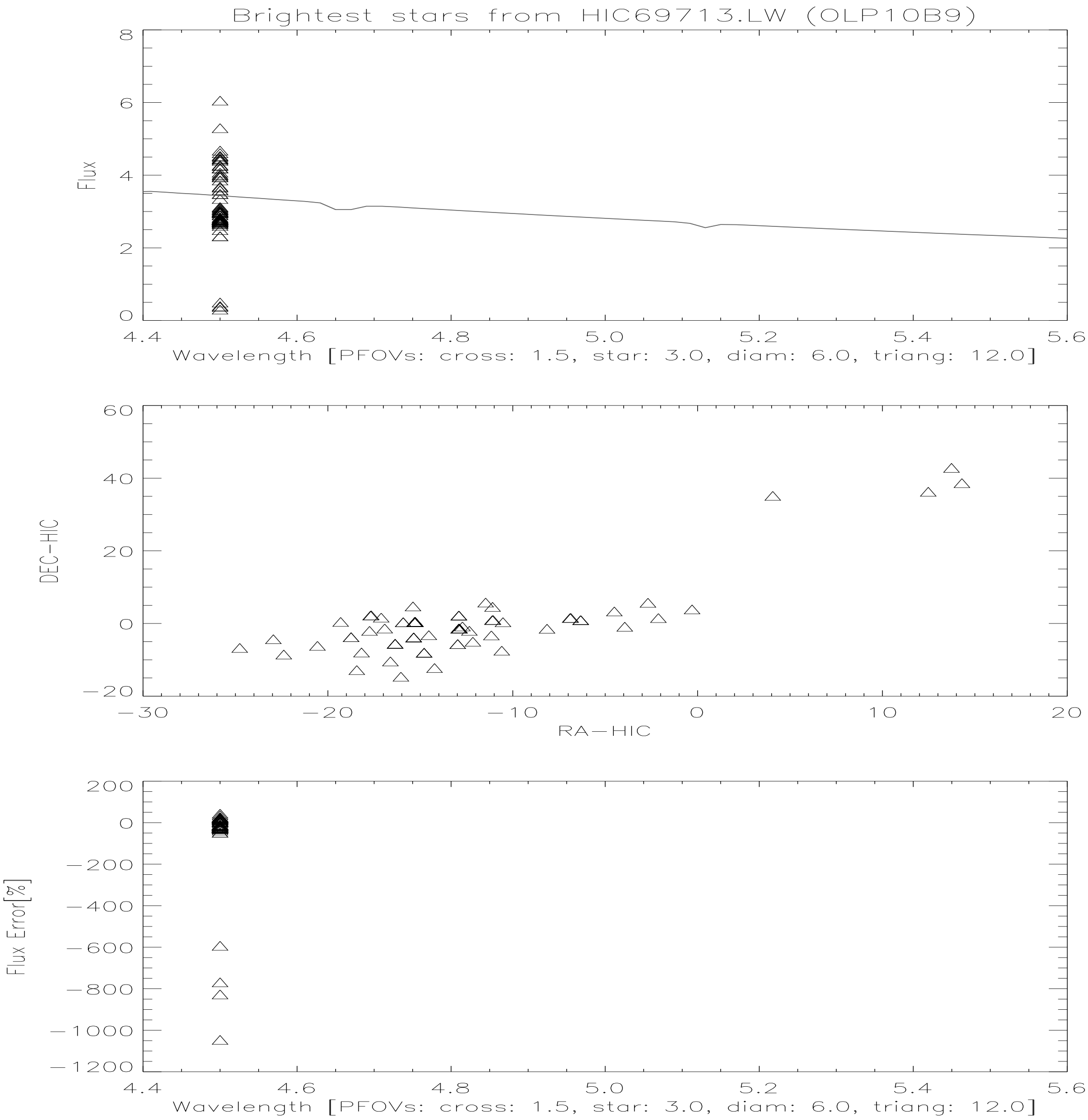

Figure 8: Plots for HIC69713 from olp10b9

TDT numbers of the observations used to create graphs and tables are: 03805455, 03805556, 03805657, 03805758, 03805859, and 03805960.

```
;Opening HIC69713.TAB
  83 stars   at 4.50E+00 mic; Flux: 3.18E+00+- 27% Error:  -7% TDT: 03805455
Grand total of   83 brights stars
Mean error this wavelength:  -7%

Mean : RA: 14h16m 8.59s DEC:   51d22m 2.3s
HIC  : RA: 14h16m 9.93s DEC:   51d22m 2.0s
DELTA: RA:-12.5 [arcsec];  DEC:  0.3 [arcsec]
```

5.3 HIC70218 - Plots and Tables

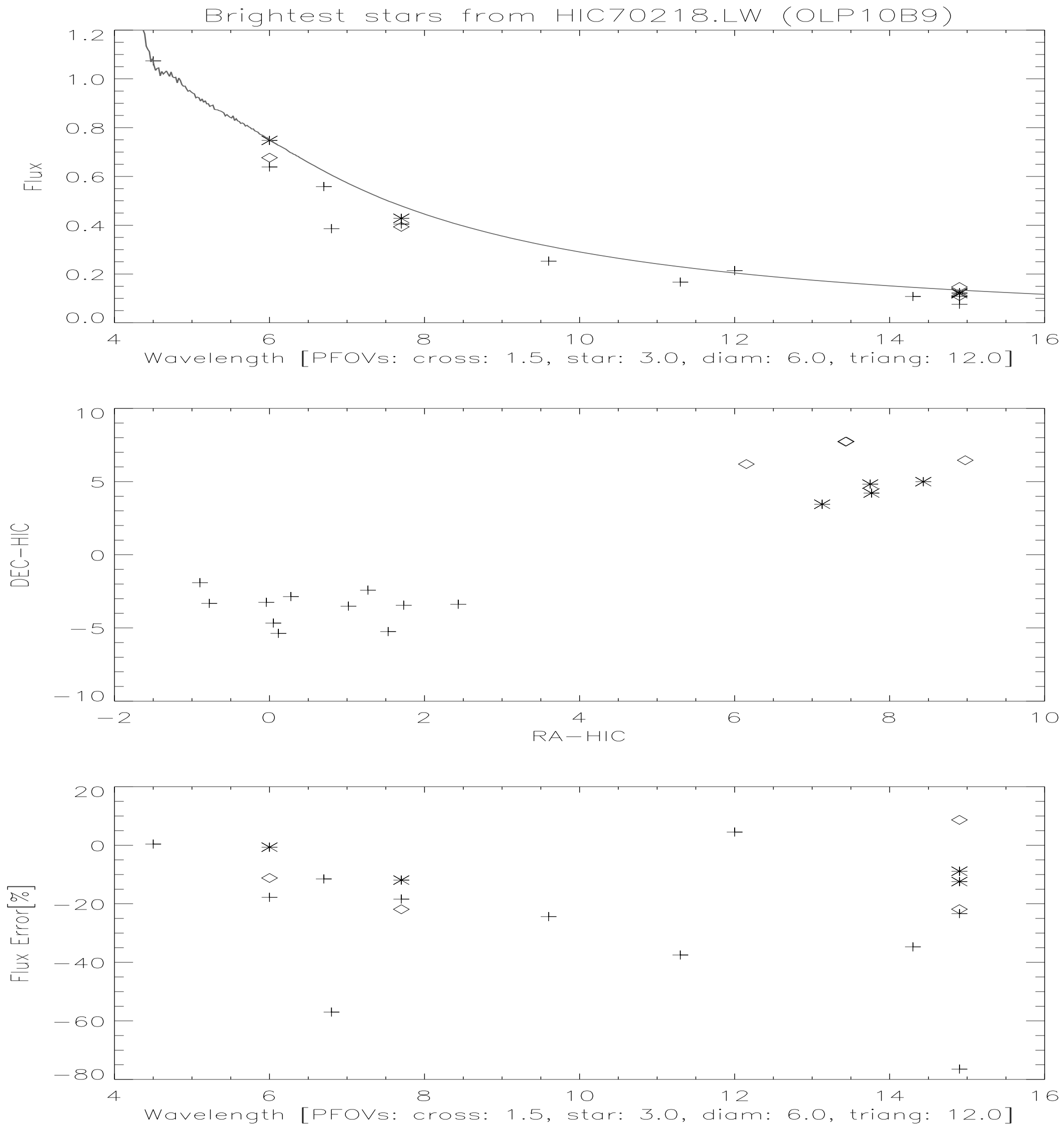

Figure 9: Plots for HIC70218 from olp10b9

TDT numbers of the observations used to create graphs and tables are: 03400802, 03401004, 03401206, 03401408, 03401509, 03401711, 03401913, 03402014, 03402115, 03402216, 03402317, 03402519, 03402721, 03402822, 03402923, 03403125, 03403327, 03403428, and 03403529.

```
Opening HIC70218.TAB
   1 stars   at 4.50E+00 mic; Flux: 1.07E+00        Error:   0% TDT: 03402216
   3 stars   at 6.00E+00 mic; Flux: 6.88E-01+-   0% Error:  -8% TDT: 03402014
   1 stars   at 6.70E+00 mic; Flux: 5.58E-01        Error: -10% TDT: 03402115
   1 stars   at 6.80E+00 mic; Flux: 3.86E-01        Error: -36% TDT: 03401408
   3 stars   at 7.70E+00 mic; Flux: 4.09E-01+-   0% Error: -14% TDT: 03401913
   1 stars   at 9.60E+00 mic; Flux: 2.53E-01        Error: -19% TDT: 03401509
   1 stars   at 1.13E+01 mic; Flux: 1.67E-01        Error: -27% TDT: 03401206
   1 stars   at 1.20E+01 mic; Flux: 2.14E-01        Error:   4% TDT: 03401711
```

```
   1 stars   at 1.43E+01 mic; Flux: 1.08E-01       Error: -25% TDT: 03401004
   6 stars   at 1.49E+01 mic; Flux: 1.14E-01+-  0% Error: -14% TDT: 03400802
Grand total of   19 brights stars
Mean error all wavelengths: -14%

Mean : RA: 14h21m57.50s DEC:   29d37m46.9s
HIC  : RA: 14h21m57.22s DEC:   29d37m46.6s
DELTA: RA:  3.6 [arcsec];  DEC:  0.3 [arcsec]
```

5.4 HIC73005 - Plots and Tables

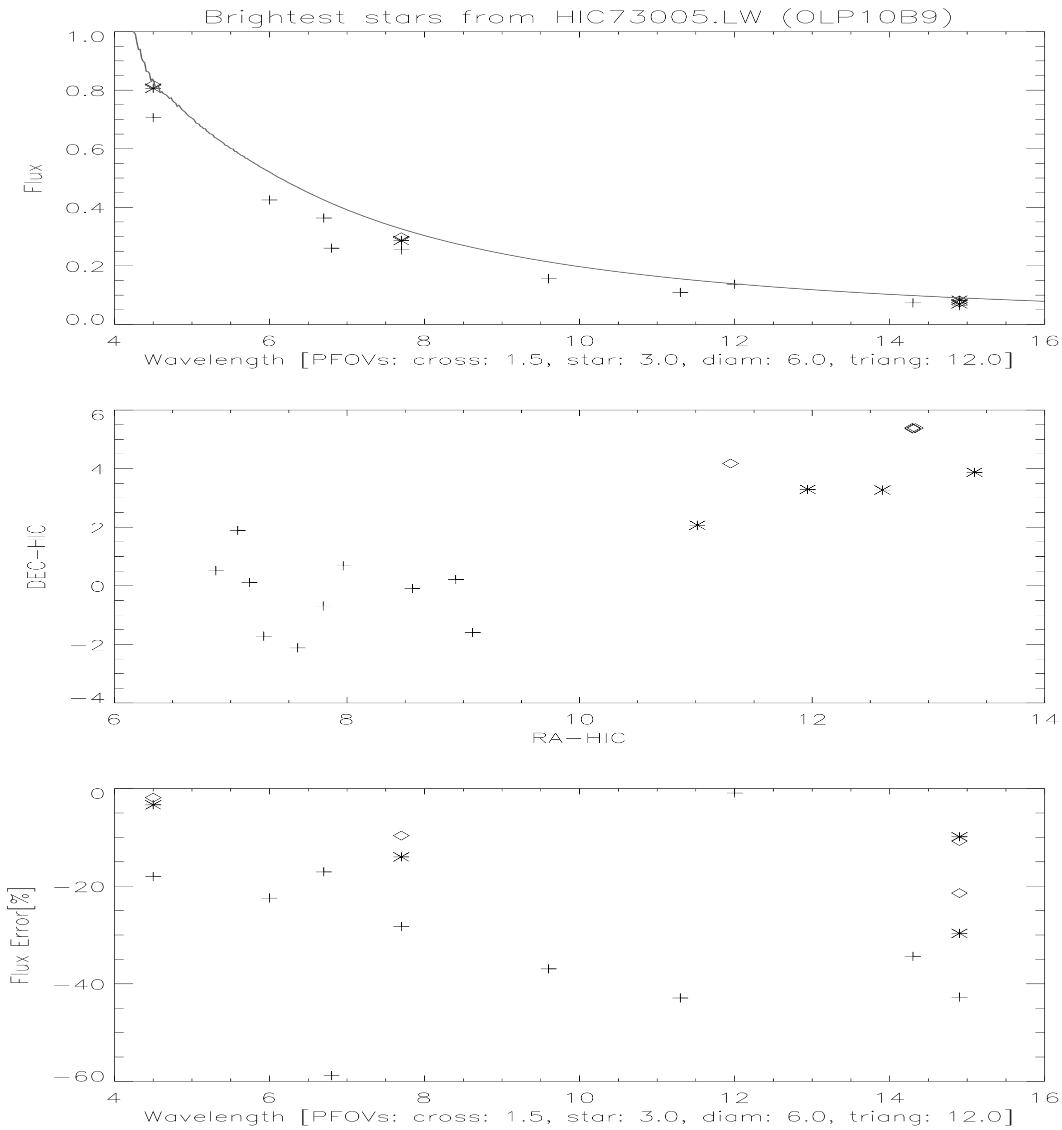

Figure 10: Plots for HIC73005 from olp10b9

TDT numbers of the observations used to create graphs and tables are: 03000502, 03000704, 03000906, 03001108, 03001209, 03001411, 03001613, 03001714, 03001815, 03001916, 03002017, 03002219, 03002421, 03002522, 03002623, 03002825, 03003027, 03003128, 03003229.

```
Opening HIC73005.TAB
   3 stars   at 4.50E+00 mic; Flux: 7.77E-01+-  0% Error:  -6% TDT: 03001916
   1 stars   at 6.00E+00 mic; Flux: 4.25E-01      Error: -18% TDT: 03001714
   1 stars   at 6.70E+00 mic; Flux: 3.63E-01      Error: -14% TDT: 03001815
   1 stars   at 6.80E+00 mic; Flux: 2.61E-01      Error: -37% TDT: 03001108
   3 stars   at 7.70E+00 mic; Flux: 2.80E-01+-  0% Error: -14% TDT: 03001613
   1 stars   at 9.60E+00 mic; Flux: 1.56E-01      Error: -26% TDT: 03001209
   1 stars   at 1.13E+01 mic; Flux: 1.09E-01      Error: -30% TDT: 03000906
   1 stars   at 1.20E+01 mic; Flux: 1.37E-01      Error:   0% TDT: 03001411
```

```
   1 stars   at 1.43E+01 mic; Flux: 7.34E-02       Error: -25% TDT: 03000704
   5 stars   at 1.49E+01 mic; Flux: 7.48E-02+-  0% Error: -17% TDT: 03002017
Grand total of   18 brights stars
Mean error all wavelengths: -18%

Mean : RA: 14h55m12.15s DEC:   53d40m50.9s
HIC  : RA: 14h55m11.04s DEC:   53d40m49.2s
DELTA: RA:  9.8 [arcsec];  DEC:  1.7 [arcsec]
```

5.5 HIC77277 - Plots and Tables

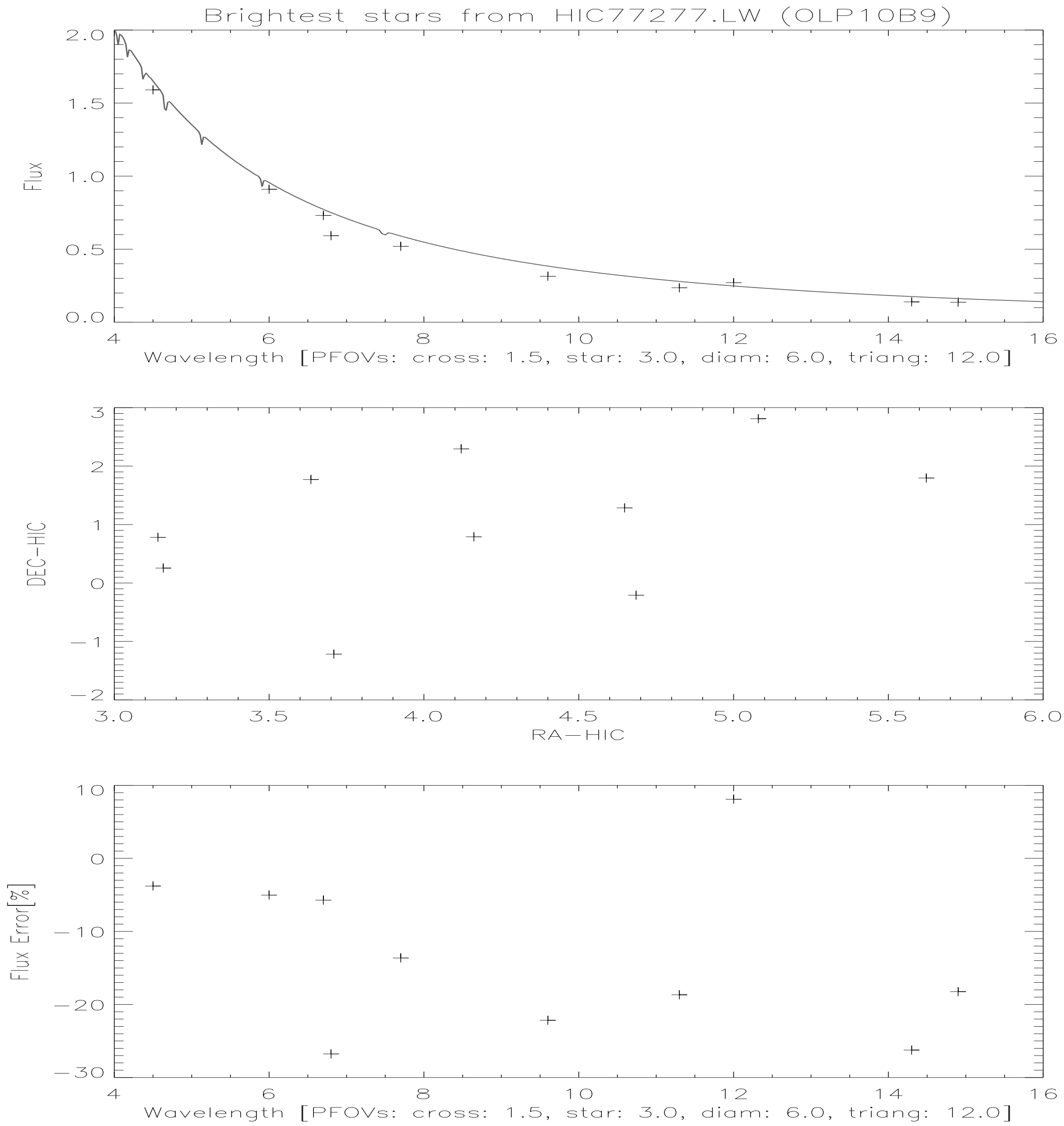

Figure 11: Plots for HIC77277 from olp10b9

TDT numbers of the observations used to create graphs and tables are: 55203131, 55203232, 55203333, 55203434, 55203535, 55203636, 55203737, 55203838, 55203939, 55204040, 55204141, 55204242, 55204343, 55204444, 55204545.

```
Opening HIC77277.TAB
   1 stars   at 4.50E+00 mic; Flux: 1.59E+00       Error:  -3% TDT: 55204242
   1 stars   at 6.00E+00 mic; Flux: 9.10E-01       Error:  -4% TDT: 55204444
   1 stars   at 6.70E+00 mic; Flux: 7.31E-01       Error:  -5% TDT: 55204343
   1 stars   at 6.80E+00 mic; Flux: 5.92E-01       Error: -21% TDT: 55203838
   1 stars   at 7.70E+00 mic; Flux: 5.19E-01       Error: -11% TDT: 55204545
   1 stars   at 9.60E+00 mic; Flux: 3.15E-01       Error: -18% TDT: 55203636
   1 stars   at 1.13E+01 mic; Flux: 2.35E-01       Error: -15% TDT: 55204040
   1 stars   at 1.20E+01 mic; Flux: 2.70E-01       Error:   8% TDT: 55203737
```

```
   1 stars   at 1.43E+01 mic; Flux: 1.39E-01       Error: -20% TDT: 55203939
   1 stars   at 1.49E+01 mic; Flux: 1.37E-01       Error: -15% TDT: 55204141
Grand total of   10 brights stars
Mean error all wavelengths: -10%

Mean : RA: 15h46m40.62s DEC:   62d35m59.4s
HIC  : RA: 15h46m40.01s DEC:   62d35m58.4s
DELTA: RA:  4.2 [arcsec];  DEC:  1.0 [arcsec]
```

5.6 HIC85317 - Plots and Tables

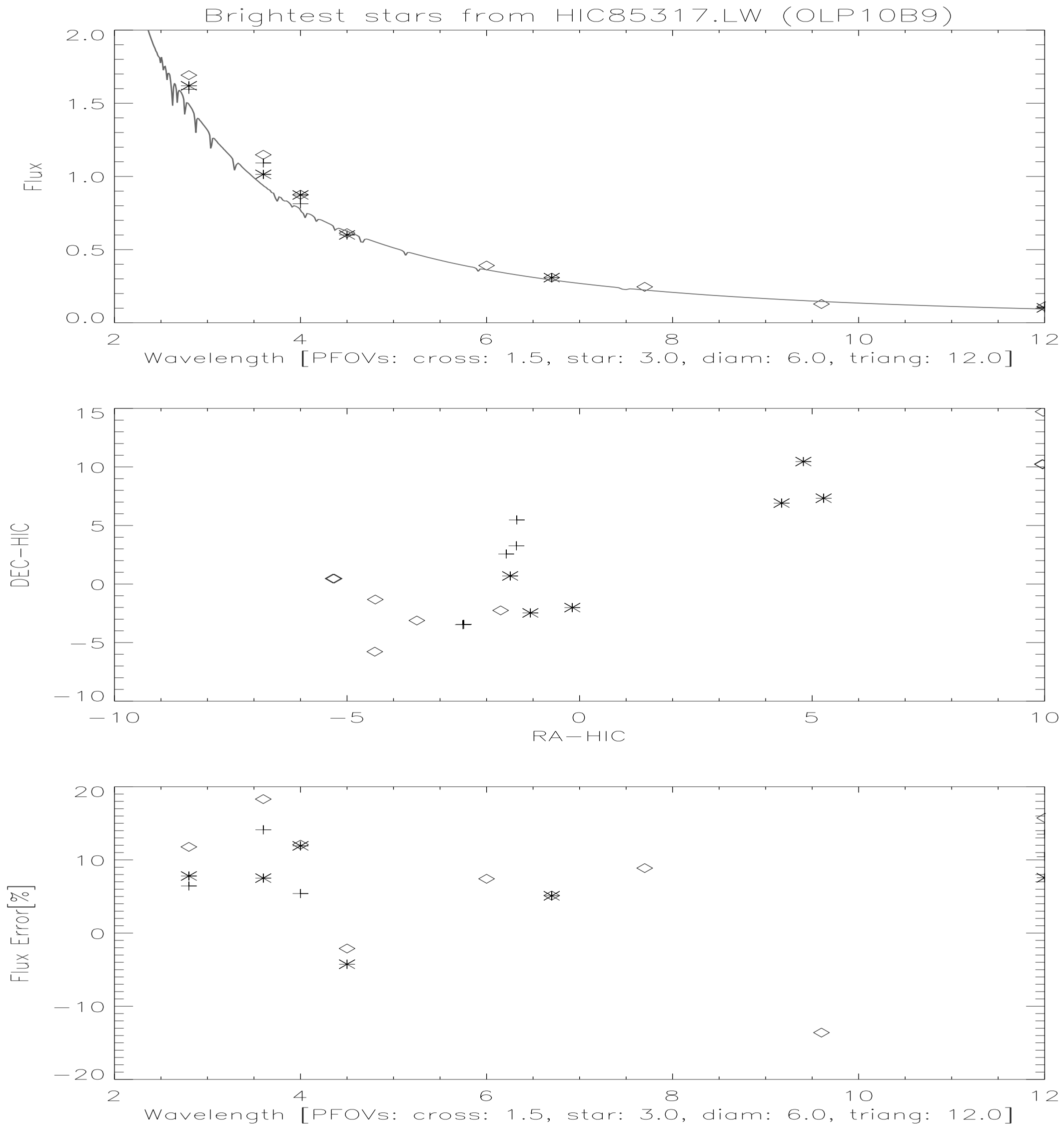

Figure 12: Plots for HIC85317 from olp10b9

TDT numbers of the observations used to create graphs and tables are: 41901802, 41901903, 41902004, 41902105, 41902206, 41902307, 41902408, 41902509, 41902610, 41902711, 41902812, 41902913, 41903023, 41903124, 41903252, 41903353, 41903454, 41903555, 41903656, 41903757, 41903858, 41903959, 41904060.

```
Opening HIC85317.TAB
   3 stars   at 2.80E+00 mic; Flux: 1.64E+00+-  0% Error:   9% TDT: 41903454
   3 stars   at 3.60E+00 mic; Flux: 1.08E+00+-  0% Error:  15% TDT: 41903353
   3 stars   at 4.00E+00 mic; Flux: 8.54E-01+-  0% Error:  10% TDT: 41903252
   2 stars   at 4.50E+00 mic; Flux: 6.06E-01+-  0% Error:  -3% TDT: 41902509
   1 stars   at 6.00E+00 mic; Flux: 3.91E-01       Error:   8% TDT: 41902408
   2 stars   at 6.70E+00 mic; Flux: 3.09E-01+-  0% Error:   5% TDT: 41902610
   1 stars   at 7.70E+00 mic; Flux: 2.46E-01       Error:   9% TDT: 41902307
   1 stars   at 9.60E+00 mic; Flux: 1.28E-01       Error: -11% TDT: 41902206
```

```
   4 stars   at 1.20E+01 mic; Flux: 1.07E-01+-  0% Error:  13% TDT: 41902105
Grand total of   20 brights stars
Mean error all wavelengths:   6%

Mean : RA: 17h26m 4.88s DEC:   58d39m 9.3s
HIC  : RA: 17h26m 4.83s DEC:   58d39m 6.8s
DELTA: RA:  0.4 [arcsec];  DEC:  2.4 [arcsec]
```

5.7 HIC94376 - Plots and Tables

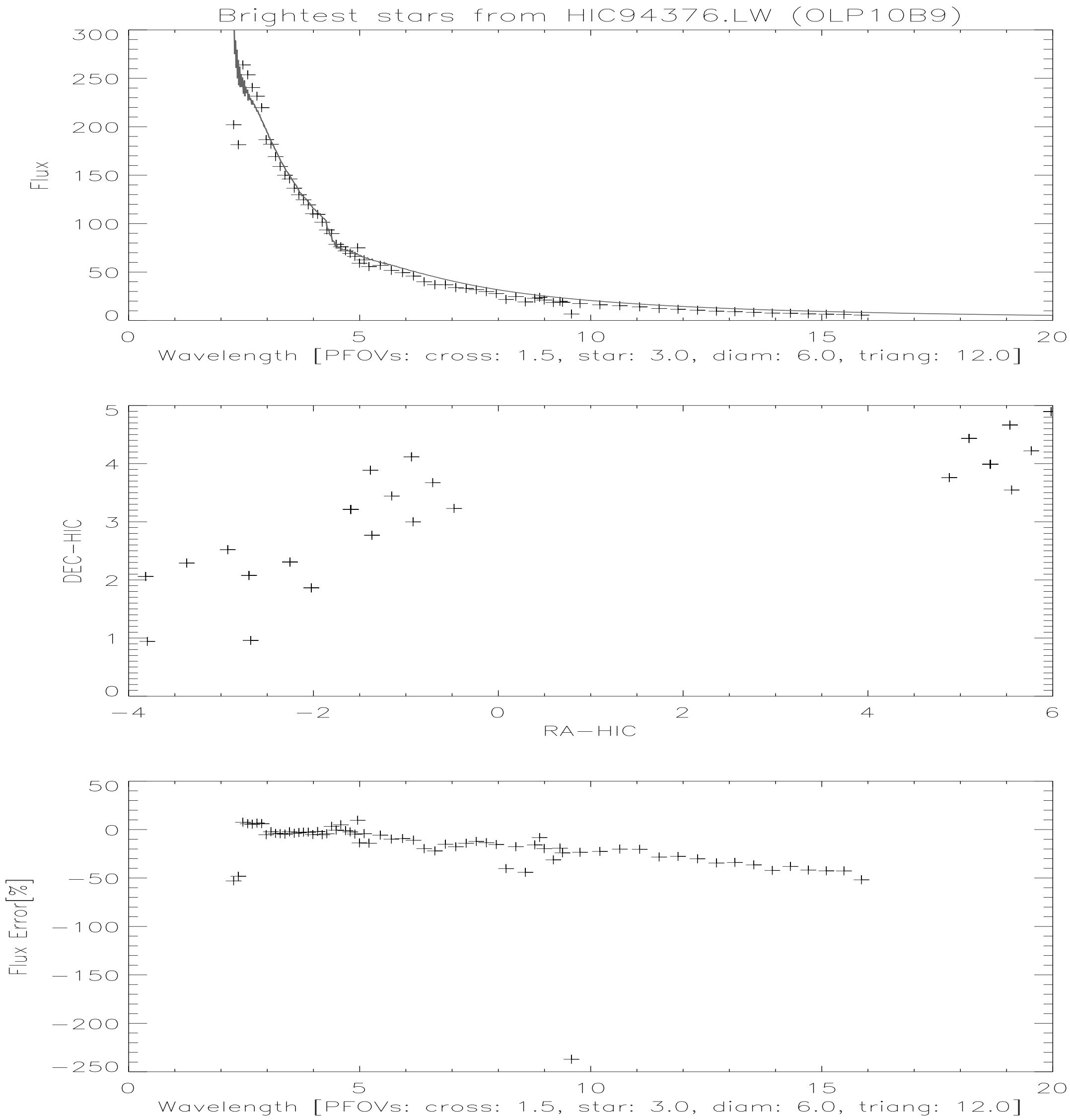

Figure 13: Plots for HIC94376 from olp10b9

TDT number of the observation used to create graphs and tables is 07807002.

```
Opening HIC94376.TAB
   1 stars   at 2.27E+00 mic; Flux: 2.02E+02       Error: -34% TDT: 07807002
   1 stars   at 2.37E+00 mic; Flux: 1.81E+02       Error: -32% TDT: 07807002
   1 stars   at 2.47E+00 mic; Flux: 2.64E+02       Error:   8% TDT: 07807002
   1 stars   at 2.58E+00 mic; Flux: 2.54E+02       Error:   6% TDT: 07807002
   1 stars   at 2.68E+00 mic; Flux: 2.40E+02       Error:   5% TDT: 07807002
   1 stars   at 2.78E+00 mic; Flux: 2.32E+02       Error:   7% TDT: 07807002
   1 stars   at 2.88E+00 mic; Flux: 2.20E+02       Error:   6% TDT: 07807002
   1 stars   at 2.98E+00 mic; Flux: 1.87E+02       Error:  -5% TDT: 07807002
   1 stars   at 3.08E+00 mic; Flux: 1.82E+02       Error:  -2% TDT: 07807002
   1 stars   at 3.18E+00 mic; Flux: 1.69E+02       Error:  -3% TDT: 07807002
```

```
1 stars   at 3.28E+00 mic; Flux: 1.59E+02       Error:  -4% TDT: 07807002
1 stars   at 3.38E+00 mic; Flux: 1.50E+02       Error:  -4% TDT: 07807002
1 stars   at 3.48E+00 mic; Flux: 1.46E+02       Error:  -2% TDT: 07807002
1 stars   at 3.58E+00 mic; Flux: 1.37E+02       Error:  -3% TDT: 07807002
1 stars   at 3.68E+00 mic; Flux: 1.30E+02       Error:  -3% TDT: 07807002
1 stars   at 3.79E+00 mic; Flux: 1.25E+02       Error:  -2% TDT: 07807002
1 stars   at 3.89E+00 mic; Flux: 1.19E+02       Error:  -2% TDT: 07807002
1 stars   at 3.99E+00 mic; Flux: 1.10E+02       Error:  -4% TDT: 07807002
1 stars   at 4.09E+00 mic; Flux: 1.10E+02       Error:  -1% TDT: 07807002
1 stars   at 4.19E+00 mic; Flux: 1.01E+02       Error:  -5% TDT: 07807002
1 stars   at 4.29E+00 mic; Flux: 9.35E+01       Error:  -4% TDT: 07807002
1 stars   at 4.39E+00 mic; Flux: 8.96E+01       Error:   3% TDT: 07807002
1 stars   at 4.49E+00 mic; Flux: 7.87E+01       Error:   0% TDT: 07807002
1 stars   at 4.59E+00 mic; Flux: 7.61E+01       Error:   5% TDT: 07807002
1 stars   at 4.69E+00 mic; Flux: 7.19E+01       Error:  -1% TDT: 07807002
1 stars   at 4.79E+00 mic; Flux: 6.92E+01       Error:  -2% TDT: 07807002
1 stars   at 4.89E+00 mic; Flux: 6.62E+01       Error:  -4% TDT: 07807002
1 stars   at 4.96E+00 mic; Flux: 7.51E+01       Error:  10% TDT: 07807002
1 stars   at 5.00E+00 mic; Flux: 5.91E+01       Error: -12% TDT: 07807002
1 stars   at 5.10E+00 mic; Flux: 6.26E+01       Error:  -4% TDT: 07807002
1 stars   at 5.20E+00 mic; Flux: 5.57E+01       Error: -12% TDT: 07807002
1 stars   at 5.45E+00 mic; Flux: 5.69E+01       Error:  -5% TDT: 07807002
1 stars   at 5.69E+00 mic; Flux: 5.17E+01       Error:  -8% TDT: 07807002
1 stars   at 5.93E+00 mic; Flux: 4.95E+01       Error:  -8% TDT: 07807002
1 stars   at 6.16E+00 mic; Flux: 4.59E+01       Error:  -9% TDT: 07807002
1 stars   at 6.40E+00 mic; Flux: 3.99E+01       Error: -16% TDT: 07807002
1 stars   at 6.63E+00 mic; Flux: 3.69E+01       Error: -18% TDT: 07807002
1 stars   at 6.86E+00 mic; Flux: 3.69E+01       Error: -13% TDT: 07807002
1 stars   at 7.08E+00 mic; Flux: 3.40E+01       Error: -15% TDT: 07807002
1 stars   at 7.30E+00 mic; Flux: 3.31E+01       Error: -12% TDT: 07807002
1 stars   at 7.52E+00 mic; Flux: 3.17E+01       Error: -10% TDT: 07807002
1 stars   at 7.74E+00 mic; Flux: 2.97E+01       Error: -11% TDT: 07807002
1 stars   at 7.96E+00 mic; Flux: 2.78E+01       Error: -13% TDT: 07807002
1 stars   at 8.17E+00 mic; Flux: 2.17E+01       Error: -28% TDT: 07807002
1 stars   at 8.38E+00 mic; Flux: 2.46E+01       Error: -15% TDT: 07807002
1 stars   at 8.59E+00 mic; Flux: 1.92E+01       Error: -30% TDT: 07807002
1 stars   at 8.79E+00 mic; Flux: 2.28E+01       Error: -13% TDT: 07807002
1 stars   at 8.89E+00 mic; Flux: 2.39E+01       Error:  -7% TDT: 07807002
1 stars   at 8.99E+00 mic; Flux: 2.11E+01       Error: -16% TDT: 07807002
1 stars   at 9.19E+00 mic; Flux: 1.85E+01       Error: -23% TDT: 07807002
1 stars   at 9.33E+00 mic; Flux: 1.98E+01       Error: -16% TDT: 07807002
1 stars   at 9.39E+00 mic; Flux: 1.88E+01       Error: -19% TDT: 07807002
1 stars   at 9.58E+00 mic; Flux: 6.65E+00       Error: -70% TDT: 07807002
1 stars   at 9.77E+00 mic; Flux: 1.75E+01       Error: -18% TDT: 07807002
1 stars   at 1.02E+01 mic; Flux: 1.62E+01       Error: -18% TDT: 07807002
1 stars   at 1.06E+01 mic; Flux: 1.53E+01       Error: -16% TDT: 07807002
1 stars   at 1.11E+01 mic; Flux: 1.41E+01       Error: -16% TDT: 07807002
1 stars   at 1.15E+01 mic; Flux: 1.23E+01       Error: -22% TDT: 07807002
1 stars   at 1.19E+01 mic; Flux: 1.16E+01       Error: -21% TDT: 07807002
1 stars   at 1.23E+01 mic; Flux: 1.06E+01       Error: -23% TDT: 07807002
1 stars   at 1.27E+01 mic; Flux: 9.62E+00       Error: -25% TDT: 07807002
1 stars   at 1.31E+01 mic; Flux: 9.10E+00       Error: -25% TDT: 07807002
1 stars   at 1.35E+01 mic; Flux: 8.41E+00       Error: -26% TDT: 07807002
1 stars   at 1.39E+01 mic; Flux: 7.62E+00       Error: -29% TDT: 07807002
```

```
   1 stars   at 1.43E+01 mic; Flux: 7.44E+00       Error: -27% TDT: 07807002
   1 stars   at 1.47E+01 mic; Flux: 6.87E+00       Error: -29% TDT: 07807002
   1 stars   at 1.51E+01 mic; Flux: 6.49E+00       Error: -29% TDT: 07807002
   1 stars   at 1.55E+01 mic; Flux: 6.17E+00       Error: -29% TDT: 07807002
   1 stars   at 1.59E+01 mic; Flux: 5.53E+00       Error: -34% TDT: 07807002
Grand total of   69 brights stars
Mean error all wavelengths: -12%

Mean : RA: 19h12m33.49s DEC:   67d39m44.8s
HIC  : RA: 19h12m33.30s DEC:   67d39m41.5s
DELTA: RA:  1.1 [arcsec];  DEC:  3.3 [arcsec]
```

5.8 HIC94890 - Plots and Tables

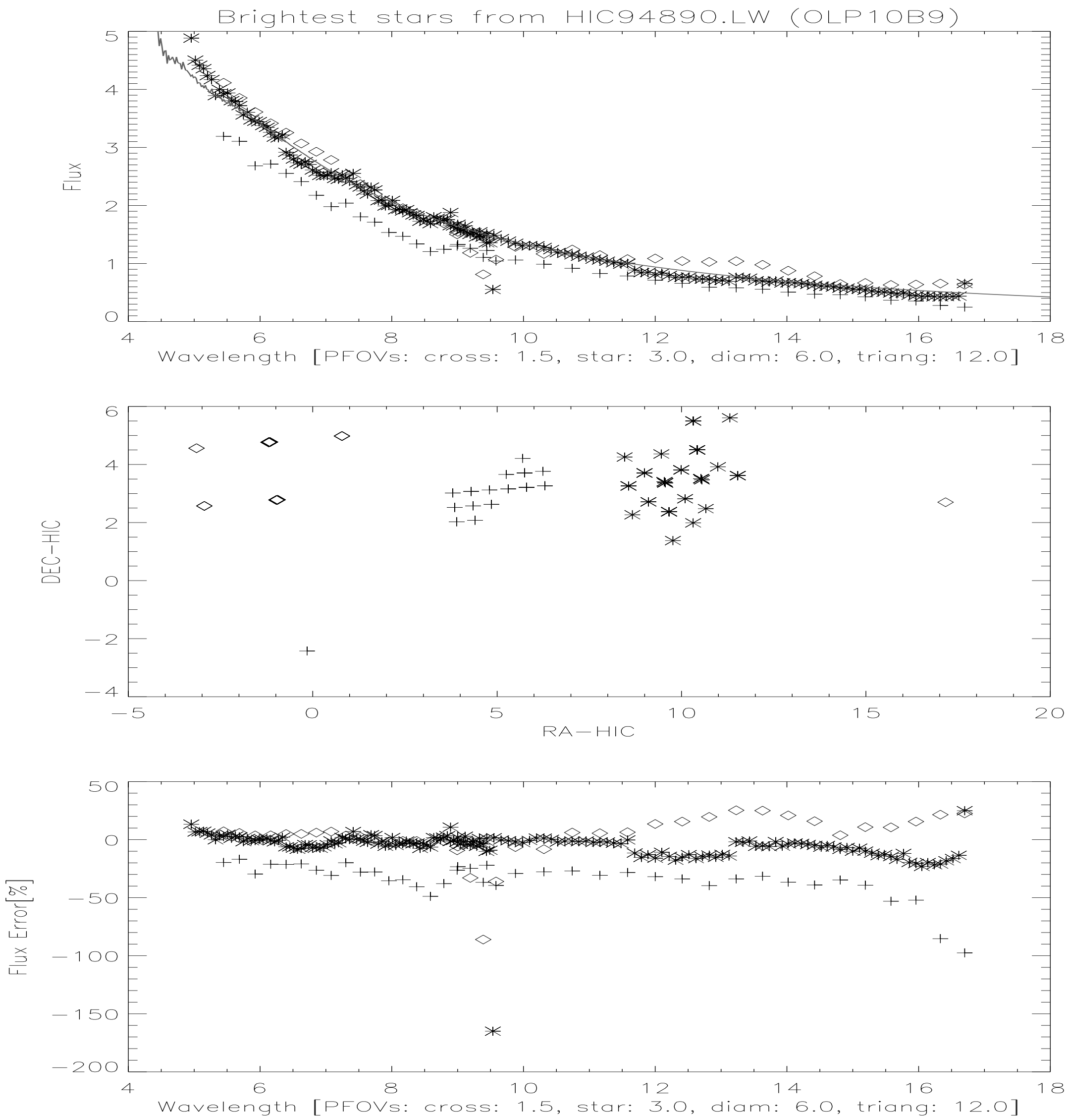

Figure 14: Plots for HIC94890 from olp10b9

TDT numbers of the observations used to create graphs and tables are: 05804802, 05804903, 05805004, 05805408, 05805509, 05805610.

```
Opening HIC94890.TAB
   1 stars   at 4.96E+00 mic; Flux: 4.88E+00       Error:  15% TDT: 05804903
   1 stars   at 5.02E+00 mic; Flux: 4.50E+00       Error:   7% TDT: 05804903
   1 stars   at 5.08E+00 mic; Flux: 4.41E+00       Error:   7% TDT: 05804903
   1 stars   at 5.14E+00 mic; Flux: 4.36E+00       Error:   7% TDT: 05804903
   1 stars   at 5.20E+00 mic; Flux: 4.24E+00       Error:   5% TDT: 05804903
   1 stars   at 5.26E+00 mic; Flux: 4.17E+00       Error:   4% TDT: 05804903
   1 stars   at 5.32E+00 mic; Flux: 3.89E+00       Error:   0% TDT: 05804903
   1 stars   at 5.39E+00 mic; Flux: 4.00E+00       Error:   3% TDT: 05804903
   3 stars   at 5.45E+00 mic; Flux: 3.74E+00+-   6% Error:  -2% TDT: 05804802
```

```
1 stars   at 5.51E+00 mic; Flux: 3.94E+00       Error:   4% TDT: 05804903
1 stars   at 5.57E+00 mic; Flux: 3.81E+00       Error:   1% TDT: 05804903
1 stars   at 5.63E+00 mic; Flux: 3.79E+00       Error:   3% TDT: 05804903
3 stars   at 5.69E+00 mic; Flux: 3.56E+00+-  4% Error:  -1% TDT: 05804802
1 stars   at 5.75E+00 mic; Flux: 3.56E+00       Error:  -1% TDT: 05804903
1 stars   at 5.81E+00 mic; Flux: 3.60E+00       Error:   1% TDT: 05804903
1 stars   at 5.87E+00 mic; Flux: 3.47E+00       Error:   0% TDT: 05804903
3 stars   at 5.93E+00 mic; Flux: 3.25E+00+-  7% Error:  -6% TDT: 05804802
1 stars   at 5.99E+00 mic; Flux: 3.44E+00       Error:   0% TDT: 05804903
1 stars   at 6.04E+00 mic; Flux: 3.38E+00       Error:   0% TDT: 05804903
1 stars   at 6.10E+00 mic; Flux: 3.35E+00       Error:   0% TDT: 05804903
3 stars   at 6.16E+00 mic; Flux: 3.13E+00+-  4% Error:  -4% TDT: 05804802
1 stars   at 6.22E+00 mic; Flux: 3.18E+00       Error:  -1% TDT: 05804903
1 stars   at 6.28E+00 mic; Flux: 3.16E+00       Error:   0% TDT: 05804903
1 stars   at 6.34E+00 mic; Flux: 3.21E+00       Error:   2% TDT: 05804903
3 stars   at 6.40E+00 mic; Flux: 2.91E+00+-  3% Error:  -6% TDT: 05804802
1 stars   at 6.45E+00 mic; Flux: 2.87E+00       Error:  -5% TDT: 05804903
1 stars   at 6.51E+00 mic; Flux: 2.80E+00       Error:  -6% TDT: 05804903
1 stars   at 6.57E+00 mic; Flux: 2.74E+00       Error:  -7% TDT: 05804903
3 stars   at 6.63E+00 mic; Flux: 2.73E+00+-  3% Error:  -6% TDT: 05804802
1 stars   at 6.68E+00 mic; Flux: 2.76E+00       Error:  -4% TDT: 05804903
1 stars   at 6.74E+00 mic; Flux: 2.71E+00       Error:  -4% TDT: 05804903
1 stars   at 6.80E+00 mic; Flux: 2.61E+00       Error:  -6% TDT: 05804903
3 stars   at 6.86E+00 mic; Flux: 2.56E+00+-  5% Error:  -6% TDT: 05804802
1 stars   at 6.91E+00 mic; Flux: 2.52E+00       Error:  -6% TDT: 05804903
1 stars   at 6.97E+00 mic; Flux: 2.51E+00       Error:  -5% TDT: 05804903
1 stars   at 7.02E+00 mic; Flux: 2.52E+00       Error:  -4% TDT: 05804903
3 stars   at 7.08E+00 mic; Flux: 2.44E+00+-  6% Error:  -5% TDT: 05804802
1 stars   at 7.14E+00 mic; Flux: 2.47E+00       Error:  -3% TDT: 05804903
1 stars   at 7.19E+00 mic; Flux: 2.45E+00       Error:  -2% TDT: 05804903
1 stars   at 7.25E+00 mic; Flux: 2.53E+00       Error:   1% TDT: 05804903
3 stars   at 7.30E+00 mic; Flux: 2.35E+00+-  2% Error:  -4% TDT: 05804802
1 stars   at 7.36E+00 mic; Flux: 2.41E+00       Error:   0% TDT: 05804903
1 stars   at 7.41E+00 mic; Flux: 2.55E+00       Error:   7% TDT: 05804903
1 stars   at 7.47E+00 mic; Flux: 2.36E+00       Error:   0% TDT: 05804903
3 stars   at 7.52E+00 mic; Flux: 2.16E+00+-  4% Error:  -6% TDT: 05804802
1 stars   at 7.58E+00 mic; Flux: 2.25E+00       Error:  -1% TDT: 05804903
1 stars   at 7.63E+00 mic; Flux: 2.20E+00       Error:  -2% TDT: 05804903
1 stars   at 7.69E+00 mic; Flux: 2.32E+00       Error:   4% TDT: 05804903
3 stars   at 7.74E+00 mic; Flux: 2.06E+00+-  4% Error:  -6% TDT: 05804802
1 stars   at 7.80E+00 mic; Flux: 2.08E+00       Error:  -3% TDT: 05804903
1 stars   at 7.85E+00 mic; Flux: 2.09E+00       Error:  -1% TDT: 05804903
1 stars   at 7.90E+00 mic; Flux: 1.99E+00       Error:  -5% TDT: 05804903
3 stars   at 7.96E+00 mic; Flux: 1.86E+00+-  3% Error: -10% TDT: 05804802
1 stars   at 8.01E+00 mic; Flux: 2.09E+00       Error:   1% TDT: 05804903
1 stars   at 8.06E+00 mic; Flux: 1.93E+00       Error:  -4% TDT: 05804903
1 stars   at 8.12E+00 mic; Flux: 1.94E+00       Error:  -2% TDT: 05804903
3 stars   at 8.17E+00 mic; Flux: 1.78E+00+-  3% Error: -10% TDT: 05804802
1 stars   at 8.22E+00 mic; Flux: 1.93E+00       Error:  -1% TDT: 05804903
1 stars   at 8.27E+00 mic; Flux: 1.88E+00       Error:  -2% TDT: 05804903
1 stars   at 8.33E+00 mic; Flux: 1.84E+00       Error:  -3% TDT: 05804903
3 stars   at 8.38E+00 mic; Flux: 1.67E+00+-  4% Error: -10% TDT: 05804802
1 stars   at 8.43E+00 mic; Flux: 1.73E+00       Error:  -7% TDT: 05804903
1 stars   at 8.48E+00 mic; Flux: 1.77E+00       Error:  -3% TDT: 05804903
```

```
1 stars   at 8.53E+00 mic; Flux: 1.73E+00       Error:  -4% TDT: 05804903
3 stars   at 8.59E+00 mic; Flux: 1.55E+00+-  5% Error: -13% TDT: 05804802
1 stars   at 8.64E+00 mic; Flux: 1.81E+00       Error:   1% TDT: 05804903
1 stars   at 8.69E+00 mic; Flux: 1.78E+00       Error:   1% TDT: 05804903
1 stars   at 8.74E+00 mic; Flux: 1.73E+00       Error:   0% TDT: 05804903
3 stars   at 8.79E+00 mic; Flux: 1.56E+00+-  4% Error:  -8% TDT: 05804802
1 stars   at 8.84E+00 mic; Flux: 1.76E+00       Error:   3% TDT: 05804903
1 stars   at 8.89E+00 mic; Flux: 1.65E+00       Error:  -1% TDT: 05804903
1 stars   at 8.89E+00 mic; Flux: 1.88E+00       Error:  11% TDT: 05805509
1 stars   at 8.94E+00 mic; Flux: 1.65E+00       Error:   0% TDT: 05804903
3 stars   at 8.99E+00 mic; Flux: 1.47E+00+-  1% Error: -10% TDT: 05804802
3 stars   at 9.00E+00 mic; Flux: 1.52E+00+-  1% Error:  -7% TDT: 05805408
1 stars   at 9.04E+00 mic; Flux: 1.56E+00       Error:  -3% TDT: 05804903
1 stars   at 9.09E+00 mic; Flux: 1.58E+00       Error:  -1% TDT: 05804903
1 stars   at 9.11E+00 mic; Flux: 1.65E+00       Error:   2% TDT: 05805509
1 stars   at 9.14E+00 mic; Flux: 1.53E+00       Error:  -3% TDT: 05804903
3 stars   at 9.19E+00 mic; Flux: 1.32E+00+-  1% Error: -16% TDT: 05804802
1 stars   at 9.22E+00 mic; Flux: 1.54E+00       Error:  -1% TDT: 05805509
1 stars   at 9.24E+00 mic; Flux: 1.53E+00       Error:  -1% TDT: 05804903
1 stars   at 9.29E+00 mic; Flux: 1.46E+00       Error:  -5% TDT: 05804903
1 stars   at 9.33E+00 mic; Flux: 1.54E+00       Error:   1% TDT: 05805509
1 stars   at 9.34E+00 mic; Flux: 1.48E+00       Error:  -3% TDT: 05804903
3 stars   at 9.39E+00 mic; Flux: 1.12E+00+-  6% Error: -25% TDT: 05804802
1 stars   at 9.44E+00 mic; Flux: 1.36E+00       Error:  -9% TDT: 05804903
3 stars   at 9.44E+00 mic; Flux: 1.38E+00+-  1% Error:  -7% TDT: 05805408
1 stars   at 9.49E+00 mic; Flux: 1.36E+00       Error:  -8% TDT: 05804903
1 stars   at 9.53E+00 mic; Flux: 5.54E-01       Error: -62% TDT: 05804903
1 stars   at 9.55E+00 mic; Flux: 1.49E+00       Error:   1% TDT: 05805509
2 stars   at 9.58E+00 mic; Flux: 1.05E+00+-  0% Error: -27% TDT: 05804802
1 stars   at 9.66E+00 mic; Flux: 1.43E+00       Error:   0% TDT: 05805509
1 stars   at 9.77E+00 mic; Flux: 1.39E+00       Error:   0% TDT: 05805509
3 stars   at 9.88E+00 mic; Flux: 1.23E+00+-  1% Error: -10% TDT: 05805408
1 stars   at 9.99E+00 mic; Flux: 1.31E+00       Error:  -2% TDT: 05805509
1 stars   at 1.01E+01 mic; Flux: 1.31E+00       Error:   0% TDT: 05805509
1 stars   at 1.02E+01 mic; Flux: 1.30E+00       Error:   1% TDT: 05805509
3 stars   at 1.03E+01 mic; Flux: 1.14E+00+-  1% Error:  -9% TDT: 05805408
1 stars   at 1.04E+01 mic; Flux: 1.24E+00       Error:   0% TDT: 05805509
1 stars   at 1.05E+01 mic; Flux: 1.19E+00       Error:  -2% TDT: 05805509
1 stars   at 1.06E+01 mic; Flux: 1.18E+00       Error:  -1% TDT: 05805509
3 stars   at 1.07E+01 mic; Flux: 1.10E+00+-  2% Error:  -5% TDT: 05805408
1 stars   at 1.08E+01 mic; Flux: 1.13E+00       Error:  -1% TDT: 05805509
1 stars   at 1.09E+01 mic; Flux: 1.11E+00       Error:  -1% TDT: 05805509
1 stars   at 1.11E+01 mic; Flux: 1.08E+00       Error:  -2% TDT: 05805509
3 stars   at 1.12E+01 mic; Flux: 1.01E+00+-  2% Error:  -6% TDT: 05805408
1 stars   at 1.13E+01 mic; Flux: 1.04E+00       Error:  -2% TDT: 05805509
1 stars   at 1.14E+01 mic; Flux: 1.01E+00       Error:  -2% TDT: 05805509
1 stars   at 1.15E+01 mic; Flux: 9.89E-01       Error:  -3% TDT: 05805509
3 stars   at 1.16E+01 mic; Flux: 9.55E-01+-  2% Error:  -5% TDT: 05805408
1 stars   at 1.17E+01 mic; Flux: 8.87E-01       Error: -10% TDT: 05805509
1 stars   at 1.18E+01 mic; Flux: 8.43E-01       Error: -13% TDT: 05805509
1 stars   at 1.19E+01 mic; Flux: 8.47E-01       Error: -11% TDT: 05805509
3 stars   at 1.20E+01 mic; Flux: 8.70E-01+-  4% Error:  -7% TDT: 05805408
1 stars   at 1.21E+01 mic; Flux: 8.34E-01       Error:  -9% TDT: 05805509
1 stars   at 1.22E+01 mic; Flux: 7.94E-01       Error: -12% TDT: 05805509
```

```
   1 stars   at 1.23E+01 mic; Flux: 7.60E-01       Error: -15% TDT: 05805509
   3 stars   at 1.24E+01 mic; Flux: 8.22E-01+-  4% Error:  -6% TDT: 05805408
   1 stars   at 1.25E+01 mic; Flux: 7.67E-01       Error: -11% TDT: 05805509
   1 stars   at 1.26E+01 mic; Flux: 7.33E-01       Error: -14% TDT: 05805509
   1 stars   at 1.27E+01 mic; Flux: 7.32E-01       Error: -12% TDT: 05805509
   3 stars   at 1.28E+01 mic; Flux: 7.83E-01+-  6% Error:  -5% TDT: 05805408
   1 stars   at 1.29E+01 mic; Flux: 7.06E-01       Error: -13% TDT: 05805509
   1 stars   at 1.30E+01 mic; Flux: 7.11E-01       Error: -11% TDT: 05805509
   1 stars   at 1.31E+01 mic; Flux: 6.92E-01       Error: -12% TDT: 05805509
   3 stars   at 1.32E+01 mic; Flux: 7.94E-01+-  6% Error:   2% TDT: 05805408
   1 stars   at 1.33E+01 mic; Flux: 7.49E-01       Error:  -2% TDT: 05805509
   1 stars   at 1.34E+01 mic; Flux: 7.46E-01       Error:  -1% TDT: 05805509
   1 stars   at 1.35E+01 mic; Flux: 7.04E-01       Error:  -5% TDT: 05805509
   3 stars   at 1.36E+01 mic; Flux: 7.44E-01+-  6% Error:   1% TDT: 05805408
   1 stars   at 1.37E+01 mic; Flux: 6.82E-01       Error:  -5% TDT: 05805509
   1 stars   at 1.38E+01 mic; Flux: 7.01E-01       Error:  -1% TDT: 05805509
   1 stars   at 1.39E+01 mic; Flux: 6.66E-01       Error:  -5% TDT: 05805509
   3 stars   at 1.40E+01 mic; Flux: 6.85E-01+-  4% Error:  -1% TDT: 05805408
   1 stars   at 1.41E+01 mic; Flux: 6.65E-01       Error:  -2% TDT: 05805509
Grand total of  242 brights stars
Mean error all wavelengths:  -4%

Mean : RA: 19h18m38.63s DEC:   49d34m13.6s
HIC  : RA: 19h18m37.87s DEC:   49d34m10.0s
DELTA: RA:  7.4 [arcsec];  DEC:  3.6 [arcsec]
```

6 Point source extraction and transient corrector

Section 3.3 introduces the current Point source detection and extraction algorithm. Here we address the question of the interaction between the algorithm and the memory transient corrections. In order to investigate this question we have run a scaled down version of AAC where the Fouks-Schubert correction was bypassed and compared the list of point like sources reported by this modified AAC to "official" point source lists. The experiment was performed on all CAM prime sources of revolutions 834 and 842, fourteen sources altogether. The main results are listed in Table 4.

The main finding from inspection of Table 4 is that the F-S correction seems to have very little incidence on the number of point sources found by AAC. If anything, fewer sources tend to be found when F–S corrections are applied. The last two columns list the Flux of the strongest source detected by AAC. It is clear that there is a tendency for memory corrected data to yield higher Fluxes. In fact a formal least square fit to the graph of $Flux_{corrected}$ versus $Flux_{corrected}/Flux_{not-corrected}$ (from Table 4) yields a zero slope line with a 1.17 linear term (i.e. a 17% increase in Flux, irrespective of the non–corrected Flux).

The set of figures (Figures 26 to 39), shown in the Appendix, attempt to show the strength and position of point sources detected with transient correction ON (the solid lines in the figures) and correction OFF (dashed lines). It can be seen that in most cases, as borne out by Table 4, F-S corrected sources show a higher Flux.

Table 4: Observations processed with AAC without F-S correction

TDT	Nb. sources (FS)	Nb. sources (no-FS)	Highest Flux (FS)	Highest Flux (no-FS)
83400166	98	105	0.8678	0.8737
83400187	78	82	0.2923	0.2784
83400220	7	8	0.0566	0.0456
83400950	2	2	0.1124	0.0872
83400951	2	2	0.1462	0.1476
83401623	39	38	0.8343	0.5106
83401648	1	1	0.0731	0.0731
83401718	4	1	0.0177	0.0108
84200216	14	13	0.2453	0.2289
84200217	4	4	1.2259	1.2038
84200218	8	3	0.0582	0.0493
84200315	3	2	0.0199	0.0236
84200709	12	17	0.2391	0.1556
84200805	59	57	0.0469	0.0464

6.1 Point source extraction: OLP vs. manual reduction

This section presents a comparison of the pipeline results of TDTs 11000101 and 11000102 (two raster observations of the southern part of ρ–Oph, made with LW2 and LW3, respectively), and the results published by Bontemps et al., 2001, A&A 372, 173.

Figures 15 and 16 show the LW2 sky map obtained by OLP (in fact the map generated by the CAM post–processor code). The first figure shows the point sources found by OLP whereas the second figure shows the LW2 detected sources extracted from the article by Bontemps et.al. Note that the A&A field of view is slightly larger than the two OLP rasters used to produce the figure (more raster observations were used by Bontemps et. al. to construct their map)

A different comparison between coordinates obtained by OLP and obtained by hand reduction of the data are presented in figures 17 and 18. OLP coordinates are represented as crosses; coordinates obtained from the hand reduction are shown as diamonds.

It is reassuring to see from inspection of figures 17 and 18 that many sources have been found both by OLP and manual data reduction. We have attempted to automatically find the set of point sources which are common to the OLP results and to the A&A results; this is necessary if we want to compare the Fluxes of same point sources, i.e. those in the OLP and the A&A sets. There are at least three reasons to expect slightly different RA,DEC coordinates - for any given same source - in each set: (1) the A&A data have been reduced taking into account the optical field distorsion (see the Caveats section), (2) the A&A astrometry sets have been re-centered to better agree with a number of optical identifications (for this effect we have corrected the OLP data set by introducing the appropriate RA,DEC shifts), and (3) the OLP data is obtained for each individual raster leg so that a given point source may appear several times in the source list and not necessarily with exactly the same coordinates nor with the same Flux.

We have seen that there is not a one–to–one correspondance between OLP and hand found point sources. To determine the relative calibration OLP vs. manual reduction we have to identify the sources seen by both methods. To carry out this search, we have created lists of OLP points sources that are within a radius R of the by–hand determined stars. The following series of Figures, 21 to 25, depict the $Flux_{OLP}$ vs. the $Flux_{manual}$ for several values of the radius R. For $Radius = 2[arcsec]$ we think that we have paired up the same point sources found by OLP and obtained from the A&A article. Notice that there seems to be a tendency for OLP to yield *lower* fluxes than the hand reduced data.

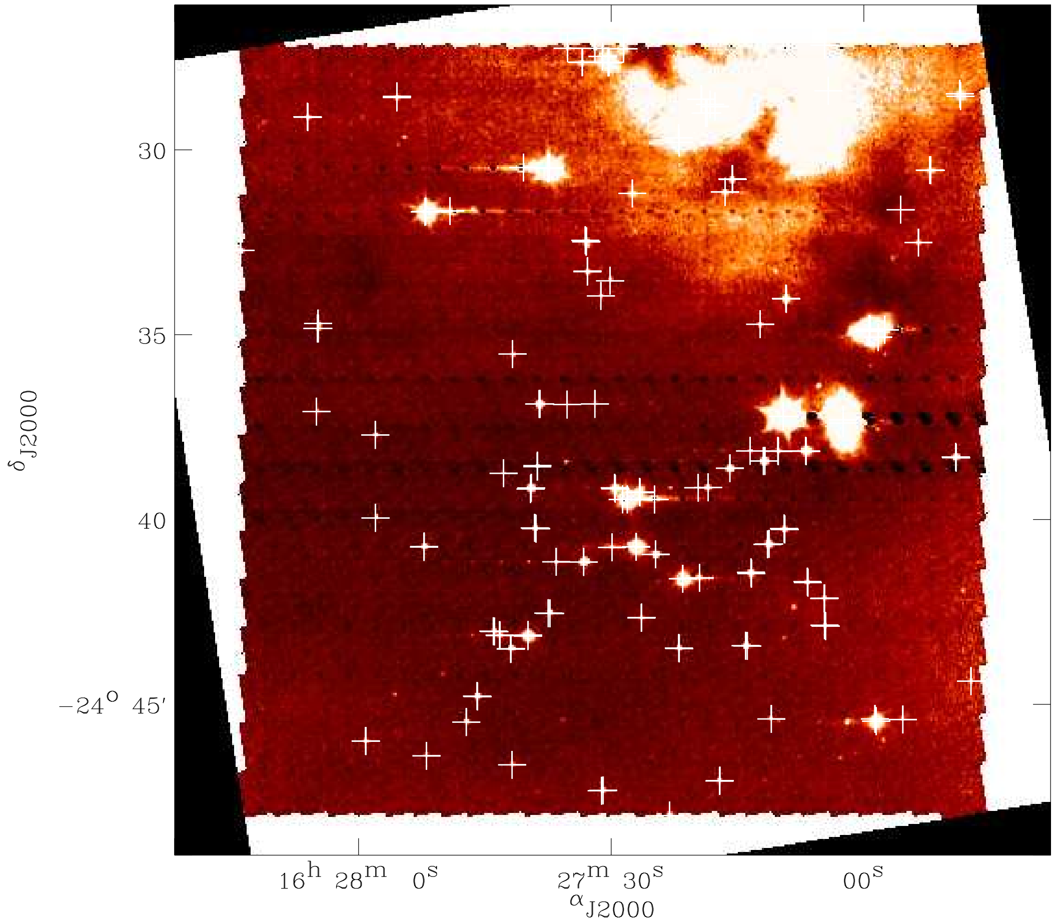

Figure 15: LW2 point sources in ρ Oph. The map and the source positions are from OLP.

7 Photometric accuracy: conclusions

A cursory look at the Tables in the previous section shows a non negligeable number of measurements falling lower than the model Flux, see the "Error:" label. This observation is borne out by the "Mean error for all wavelengths" associated to each table:

1. HIC73005 (Data used are from revolution 030). Mean error all wavelengths: -18% (was -22%)
2. HIC70218 (Data used are from revolution 034). Mean error all wavelengths: -14% (was -20%)
3. HIC69713 (Data used are from revolution 038). Mean error this wavelength: -7% (was -35%)
4. HIC94890 (Data used are from revolution 058). Mean error all wavelengths: -4% (was -8%)
5. HIC94376 (Data used are from revolution 078). Mean error all wavelengths: -12% (was -17%)
6. HIC67485 (Data used are from revolution 419). Mean error all wavelengths: 2% (was -5%)
7. HIC85317 (Data used are from revolution 419). Mean error all wavelengths: 6% (was -11%)
8. HIC77277 (Data used are from revolution 552). Mean error all wavelengths: -10% (was -17%)

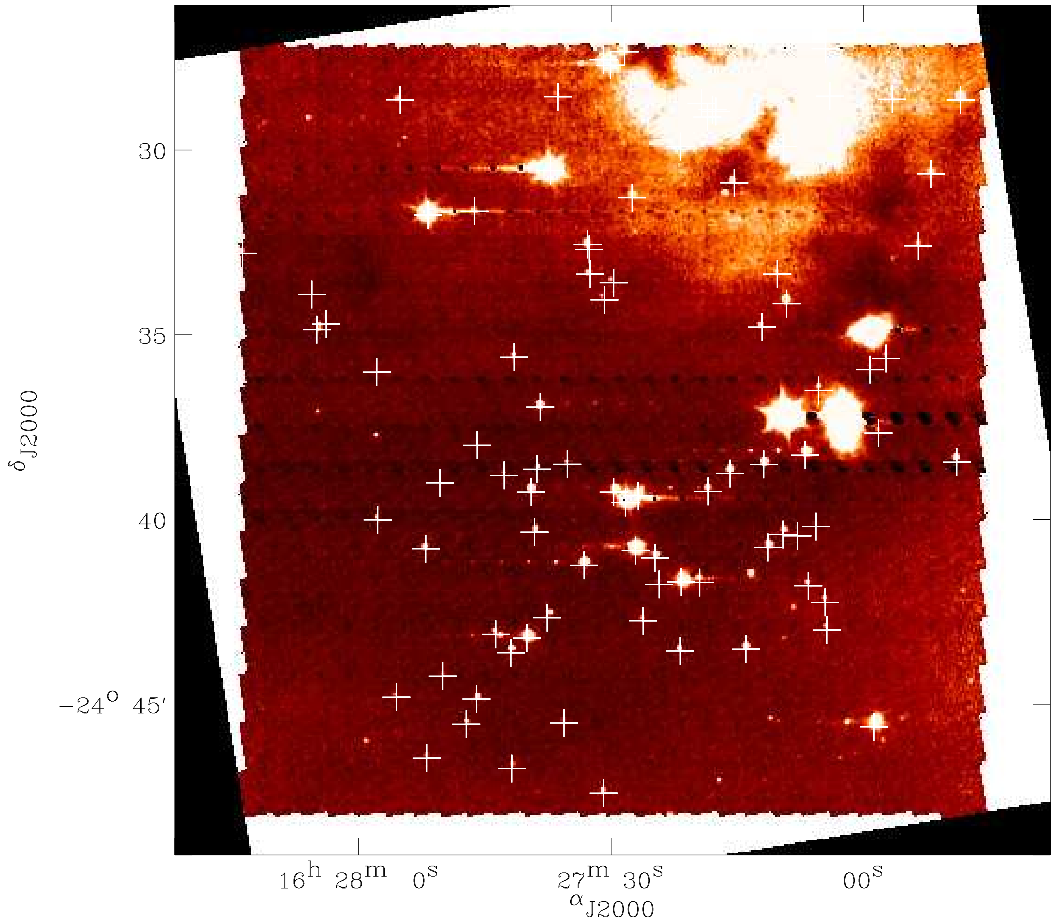

Figure 16: As figure 15 except that the sources are extracted from the article by Bontemps et al, 2001, A&A, 372, 173. Note that the sources appear to be offset to the south of the OLP map. The reason is that Bontemps et.al. have corrected the astrometry on the basis of optically identified sources.

It is worth noticing that the newer Point Source locator algorithm has indeed reduced the error figure, i.e. $Error_{Flux} = Flux_{observed} - Flux_{model}$

7.1 Important note regarding HIC-star observations

Not all the calibration observations analyzed here have been performed under identical observing circumstances. As part of the "learning curve", later observations were performed under conditions supposed to allow a better stabilisation of the detector and this is the reason why we have ordered the above list by increasing revolution number. It is not clear that there is any trend for the error to diminish with increasing revolution number, either with or without memory transient correction. If anything, a formal least-square fit to *error vs. revolution* yields a positive slope result. Many user observations were obtained not necessarily allowing for the recommended stabilisation time. Hence, the errors found above for the calibration HIC stars should be representative of the errors to be expected from the general user archived observations, for which the preconized observing rules adopted for the later calibration observations, were not necessarily followed.

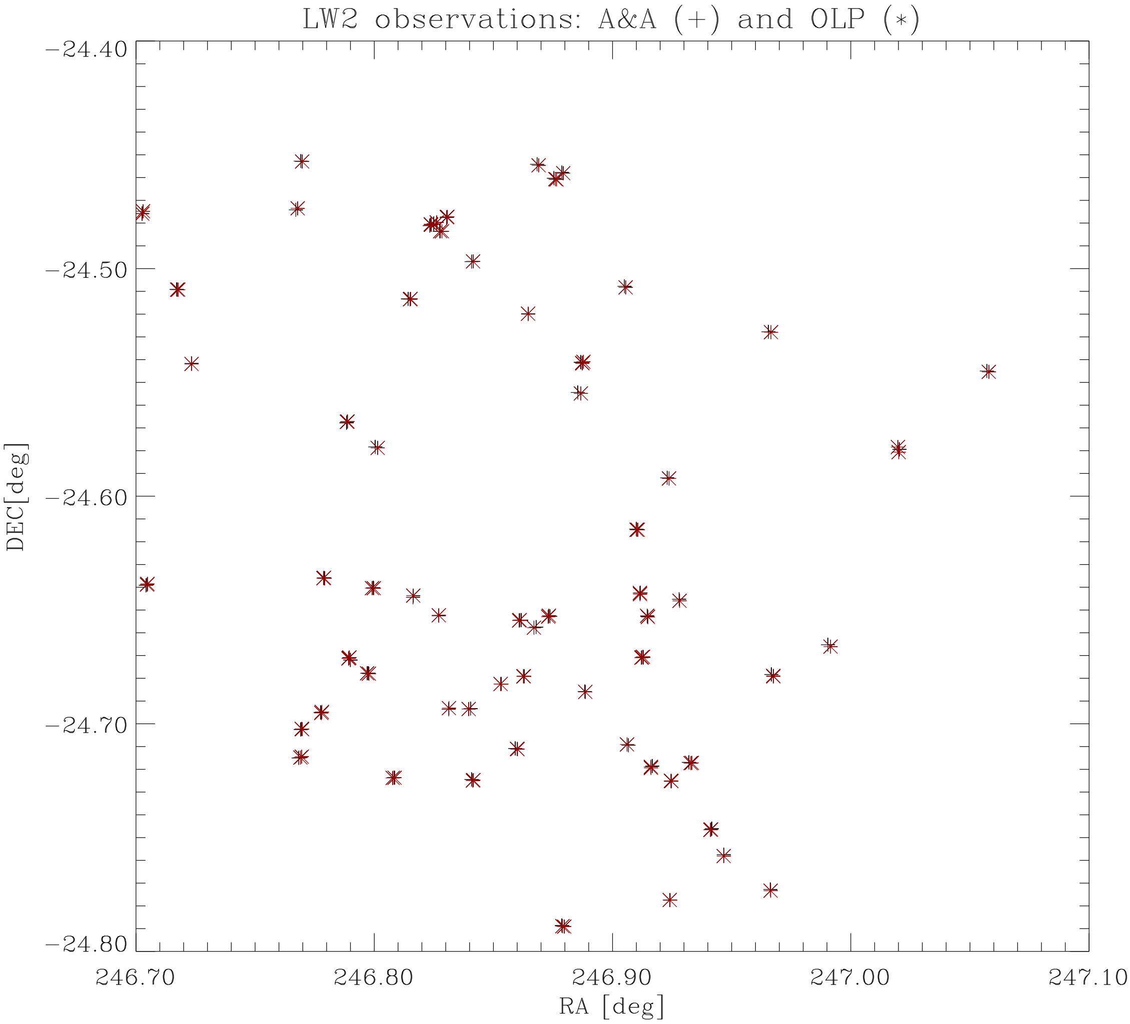

Figure 17: LW2 point sources in ρ Oph. Crosses denote point source coordinates estimated by OLP, diamonds represent the coordinates from the article by Bontemps et al, 2001, A&A, 372, 173. Common point sources (within 5 arcsec) are plotted.

8 Caveats for olp10b9 products

ISO's off–line processing has three levels of processing, resulting in several intermediate and final products. The description below applies particularly to ISOCAM data[1] (other ISO instruments apply different processing levels before generating intermediate products)

- Raw telemetry to edited telemetry. Intermediate products include: CIERtdtnb.FITS[2], (CPERtdtnb.FITS for the parallel observations) CSTAtdtnb.FITS, IIPHtdtnb.FITS, IRPHtdtnb.FITS, etc.
- Edited telemetry to ISOCAM raw images and calibrated engineering parameters. Intermediate product: CISPtdtnb.FITS (CPSPtdtnb for the parallel observations)
- Raw images to "astronomical" images and ancillary information. Products: CCIMtdtnb.FITS, CMAPStdtnb.FITS, CMOStdtnb.FITS, etc.

[1] Please refer to the ISO Data Products document for explanation of contents and layout of data products
[2] The notation tdtnb represents the eight–digit part of products' names.

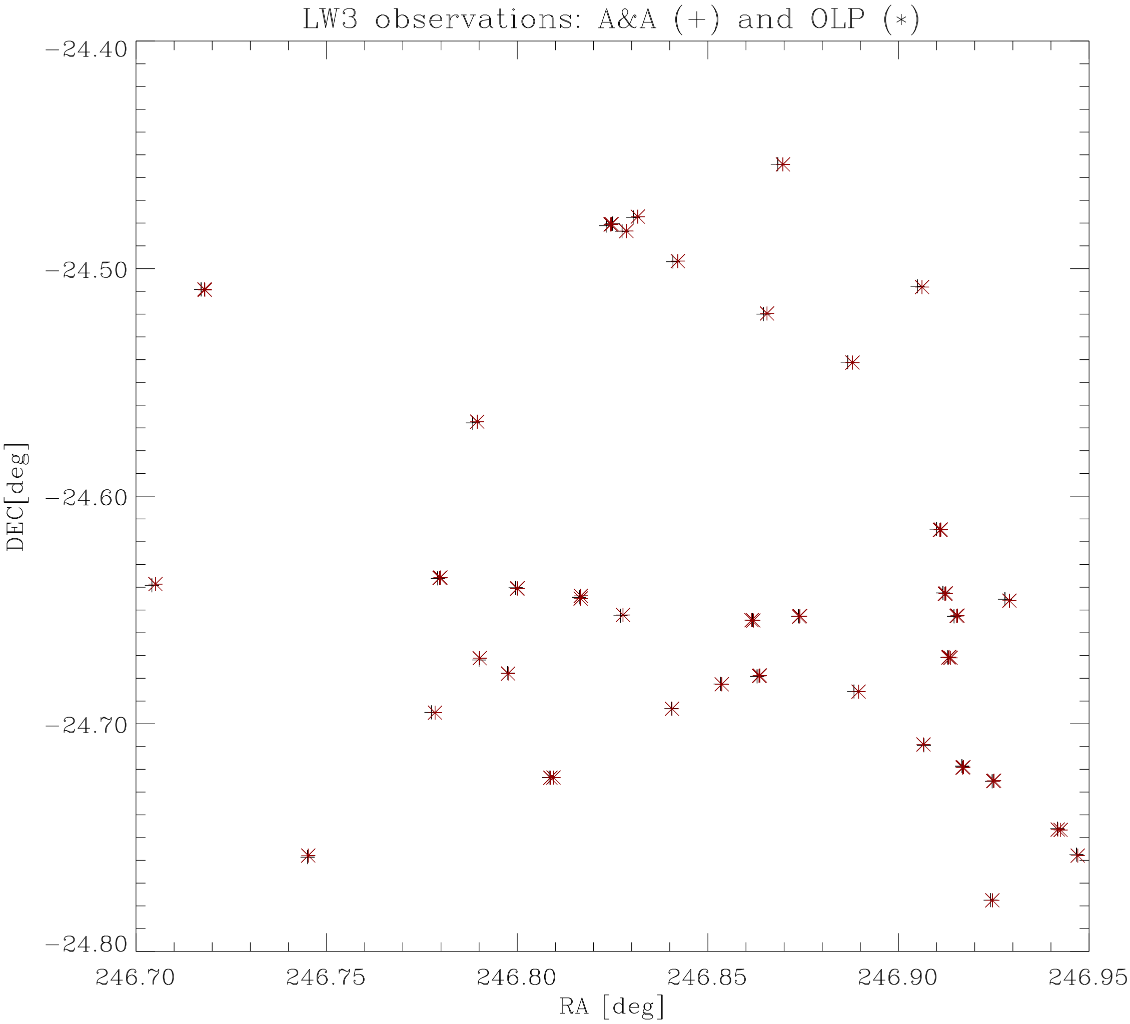

Figure 18: As figure 17 but for the LW3 detections

8.1 First processing level

Major products created here are CIER, CPER, IIPH, IRPH, and CSTA files.

8.1.1 CSTA files

Please note that the keyword CSTAREAD indicates *the number of readouts*, not to be confused with *the number of frames*. The number of frames is identical to the number of readouts only for on–board processing mode. Else, there are twice as many readouts as frames: an End of Integration and a RESET readout are needed to compute a frame. As indicated in the discussion of SCREWs, the partial implementation of SCREW301 may cause the absence of configuration records in the CSTA file of the very few observations that were affected by telemetry dropouts at the precise moment ISOCAM was being reconfigured.

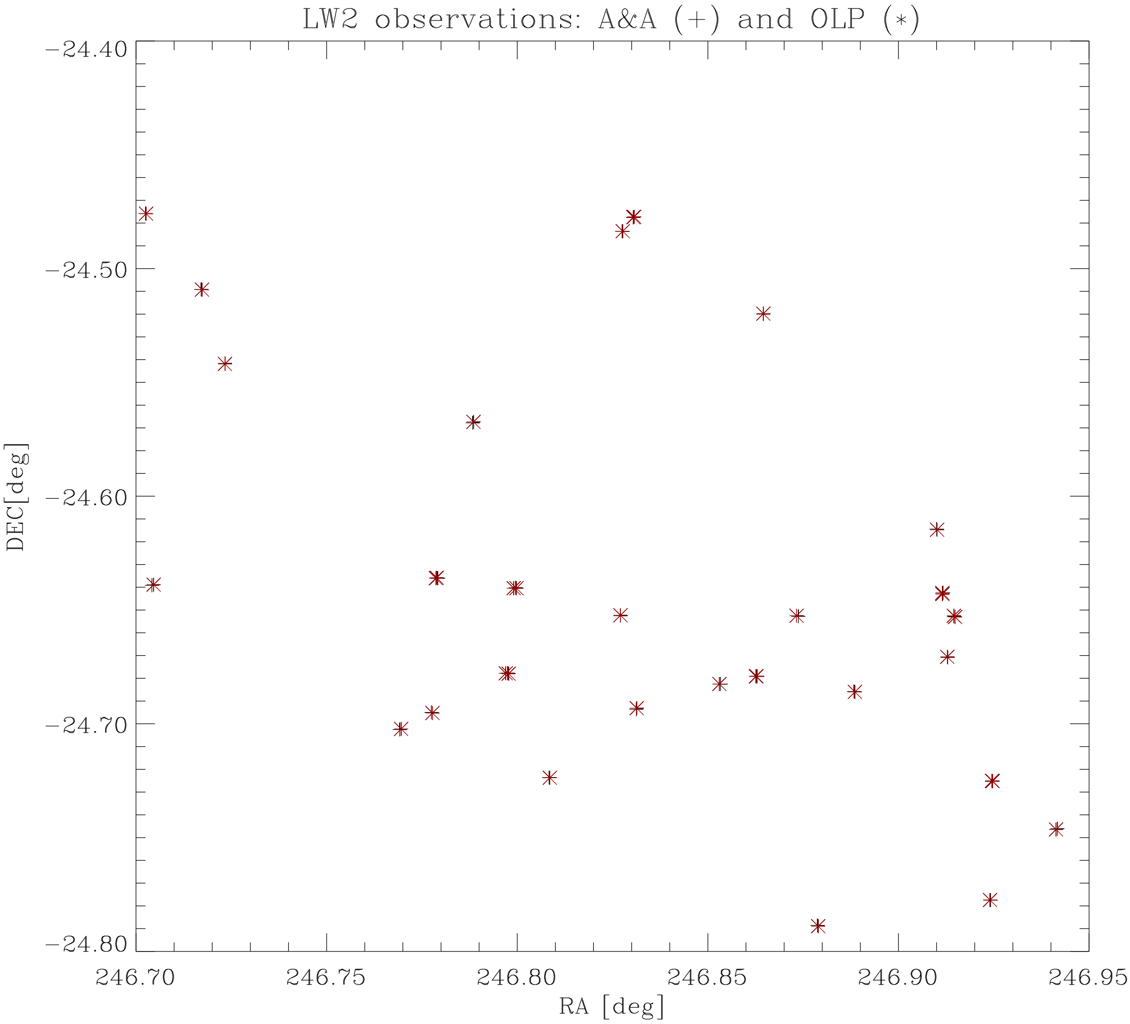

Figure 19: Common OLP-A&A LW2 point sources in ρ Oph. Crosses denote point source coordinates estimated by OLP, diamonds represent the coordinates from the article by Bontemps et al, 2001, A&A, 372, 173

8.1.2 IIPH files

Beware of occasional bumps in the IIPH during stable pointing that have been traced to the effects of cosmic ray glitches in the star tracker's CCD. Recognition of events of this type may be helped by the fact that large apparent excursions in the pointing direction are not accompanied by the OTF going down.

8.2 Second processing level

Major products created here are CISP and CPSP.

8.2.1 CISP/CPSP files

There are no known problems with the CISP (prime instrument data) and the CPSP (parallel mode data) products.

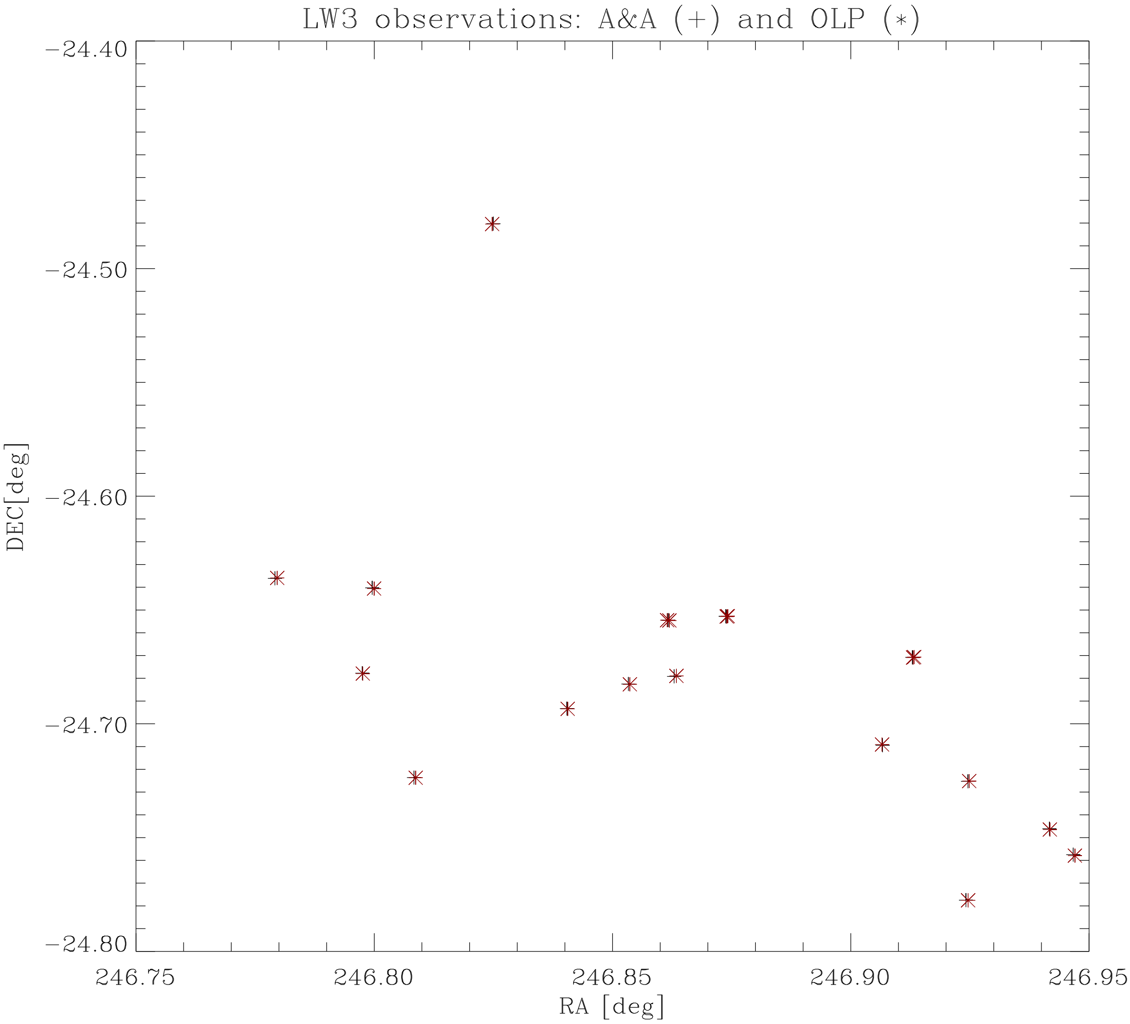

Figure 20: As figure 19 but for the LW3 detections

8.3 Third processing level

Major products created here are CCIM, CMAP, and CMOS for the images and CPSL for the point source extraction and measurement algorithm.

AAC - Automatic Analysis CAM - is an automatic procedure intended to give the astronomer a set of useful data products for his/hers research work. Every effort is made to ensure that these are as reliable and accurate as possible, including up–to–date calibrations and data reduction algorithms. However, detailed and quantitative interpretation leading to publications will generally demand the more flexible and specific scrutiny tools available to interactive analysis packages, like for example ISOCAM's CIA interactive package.

The AAC products have the "right look" when visualized on a computer screen or printed out using colour print devices. Quite often AAC images cannot be told apart from interactive analysis produced images. We believe they can safely be used as overlays for comparison with other type of data, i.e. radio, optical, etc. It is believed that equatorial coordinates reported by AAC are correct to $3 \times PFOV + 3$ (arcsec) (but see figure 16 and following paragraphs on astrometrical precision).

Scientific use of CAM data products based on OLP results requires the exercise of caution on account of the following shortcuts:

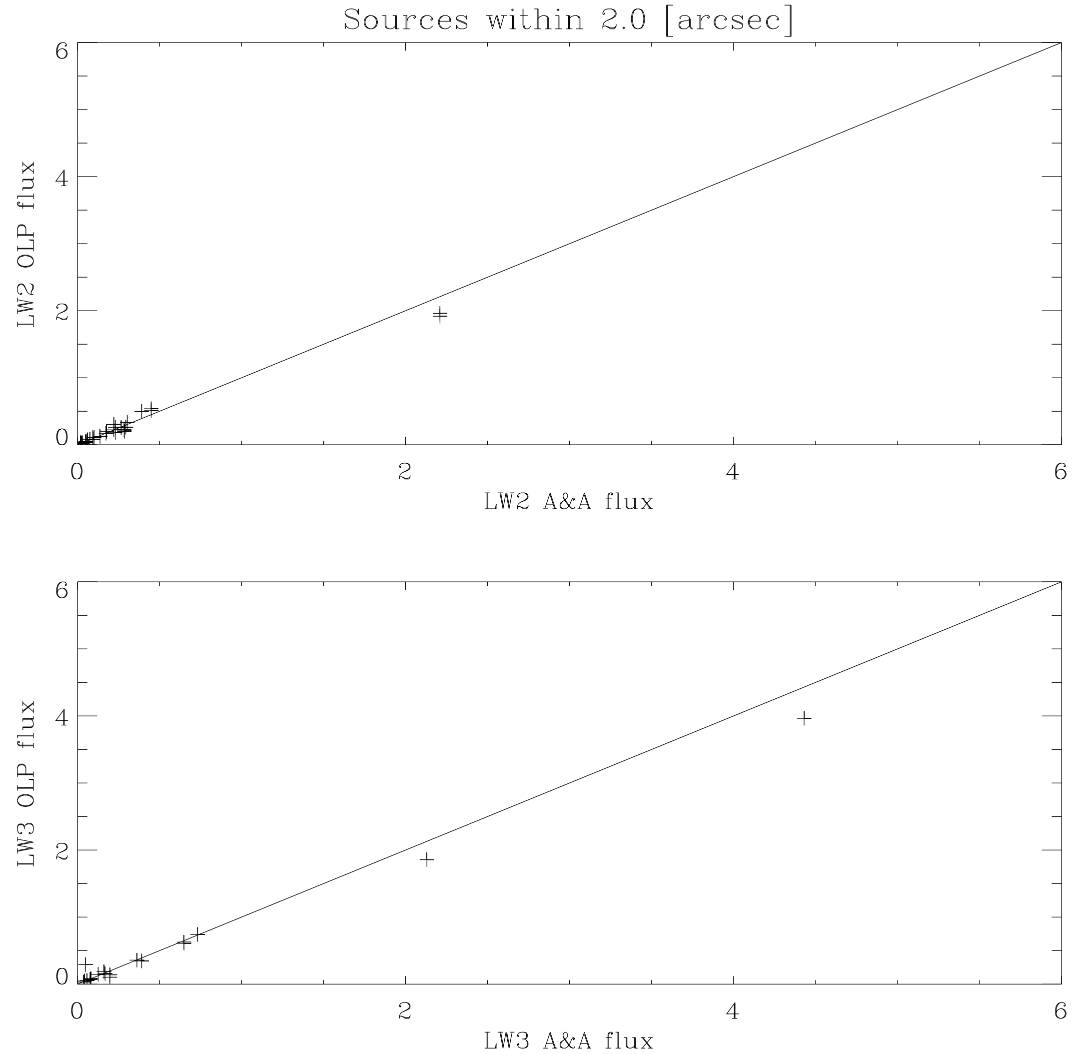

Figure 21: Fluxes of point sources in ρ Oph found by OLP and obtained from the hand–reduction of A&A.

1. AAC uses only time–independent flat–field corrections as available in the CAL–G libraries, leading to the possibility of less accurate Fluxes compared with those calculated using optimised flat corrections as currently done within CIA. The likely outcome is poor Flux calibration at the edges of the field of view.

2. AAC uses the Fouks–Schubert formalism to correct for transient effects. The method is applied only to LW data - except CAM parallel observations. The algorithm is applied blindly, i.e. the needed quiescent level at the beginning of the observations is not necessarily the most appropriate value. In some extreme cases this can lead to completely wrong predictions of the corrected data. Note also that the current algorithm breaks down for point like sources. However, the data is not "ruined", it just remain uncorrected.

3. Repositioning accuracy of the lens- and filter wheels is not taken into account. The penalty is flat–fielding and minor coordinate errors, typically less than 2 pixels. This effect is quite visible on the HIC point sources found included in the Validation Report were more often than not the [RA, DEC] deviations from the mean appear as two distinct swarms of points.

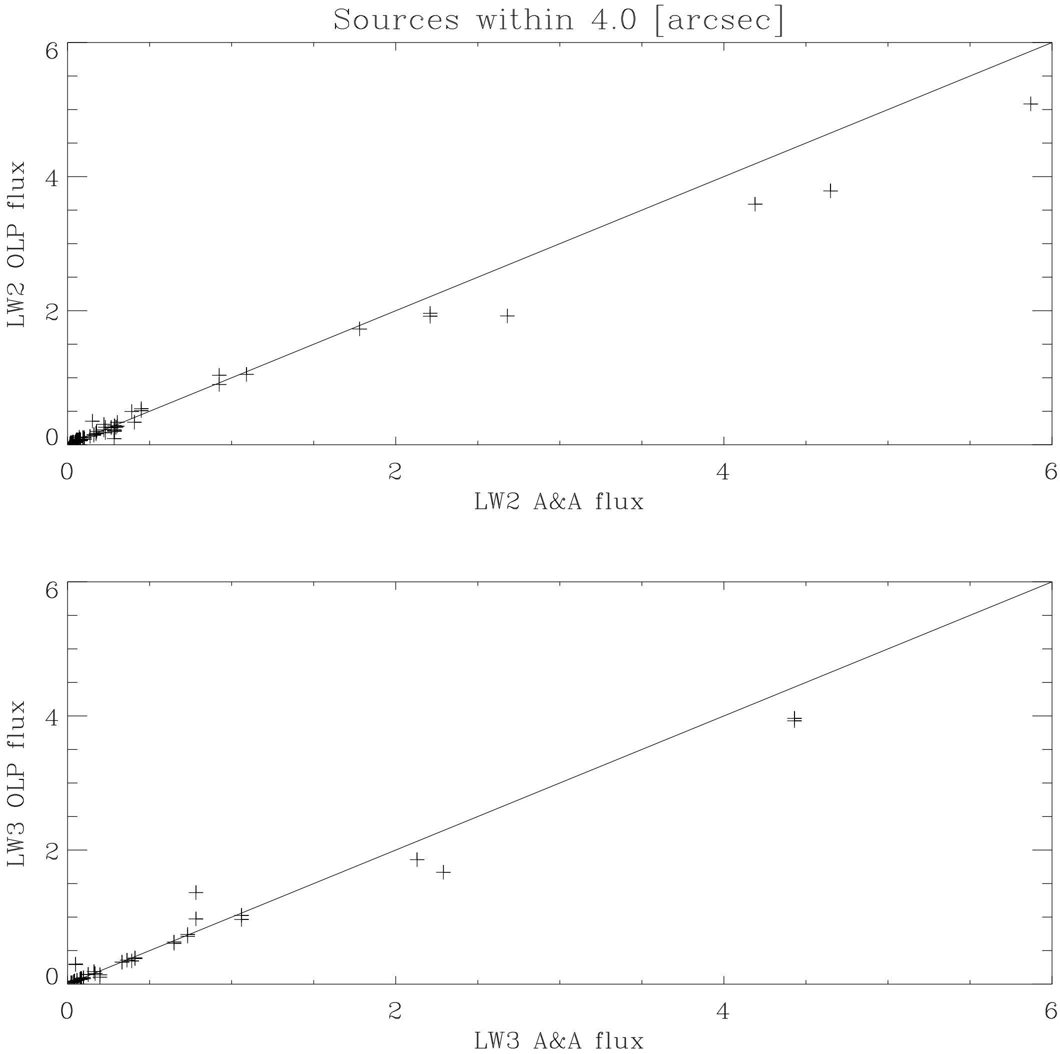

Figure 22: Fluxes of point sources in ρ Oph found by OLP and obtained from the hand–reduction of A&A.

4. Bending of ISOCAM optical axis as a function of filter or of CVF position is not considered. This leads to coordinate errors of up to one pixel.

5. The quantification of the optical distortion away from the optical centre is not included in the OLP code; leads to celestial position and integrated Flux errors; see discussion in the IDUM.

6. Varying CVF effective wavelength away from the optical centre; leads to wavelength errors amounting to the equivalent of one CVF step.

7. AAC makes no straylight or ghost corrections leading to the possibility of Flux errors and the detection of spurious sources.

8. Errors reported by AAC in the CPSL product are only statistical and take no account of any systematic effects.

9. Observations performed near the extremes of the CVF ranges, i.e. outside the range recommended in the Cookbook, are less accurately calibrated.

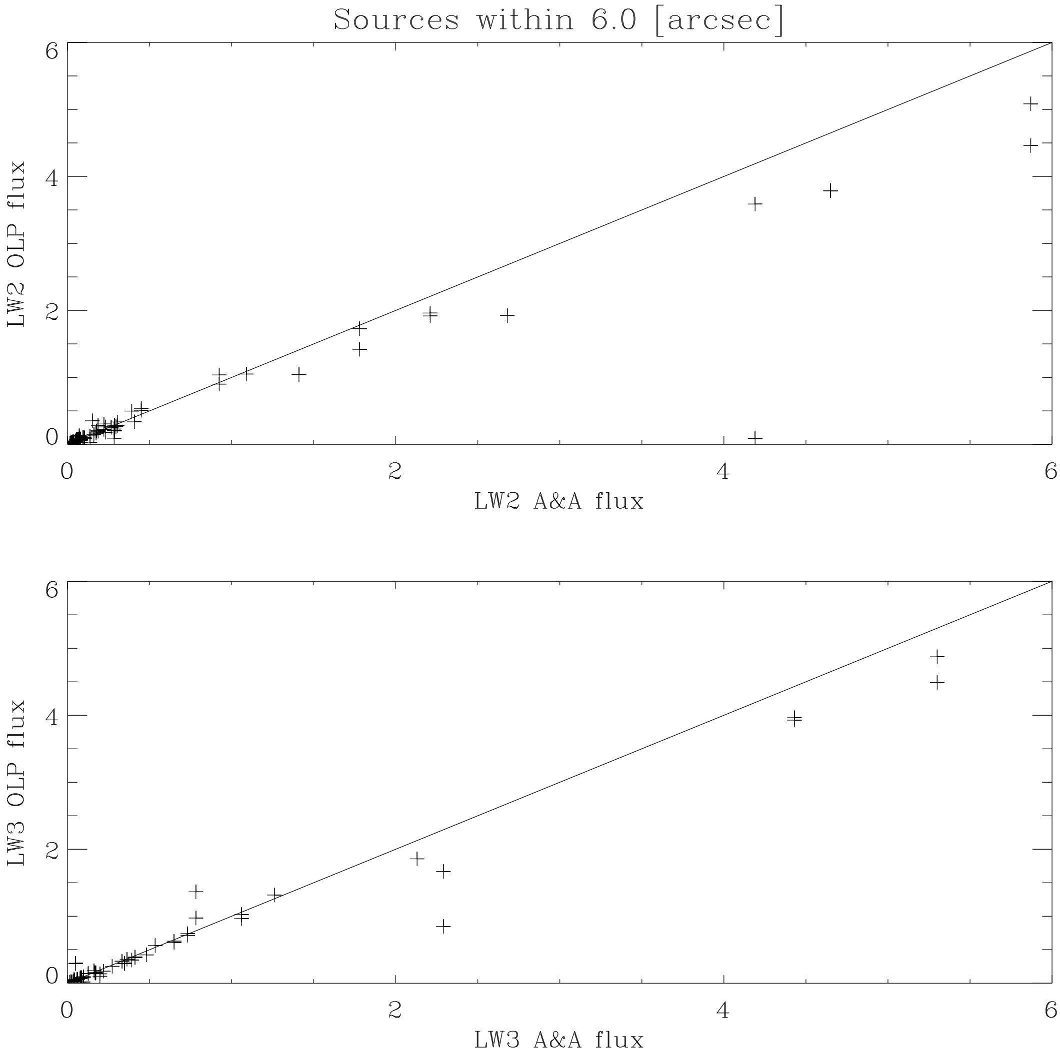

Figure 23: Fluxes of point sources in ρ Oph found by OLP and obtained from the hand–reduction of A&A.

10. Non-linearity of detectors is not taken into account. This affects in particular the SW detector when a very bright point source is observed.

The observer should bear in mind the above shortcuts when assessing the contents of the individual AAC products discussed below.

8.3.1 CCIM files

There are no relevant caveats associated to these files.

8.3.2 CMAP products

- CMAPs are constructed using the reference celestial coordinates from the IRPH files with no correction for the IIPH pointing jitter, which as discussed above, is of amplitude small enough to be dominated by measurement noise, but still large enough to give image blur of about 1 arcsec in size.

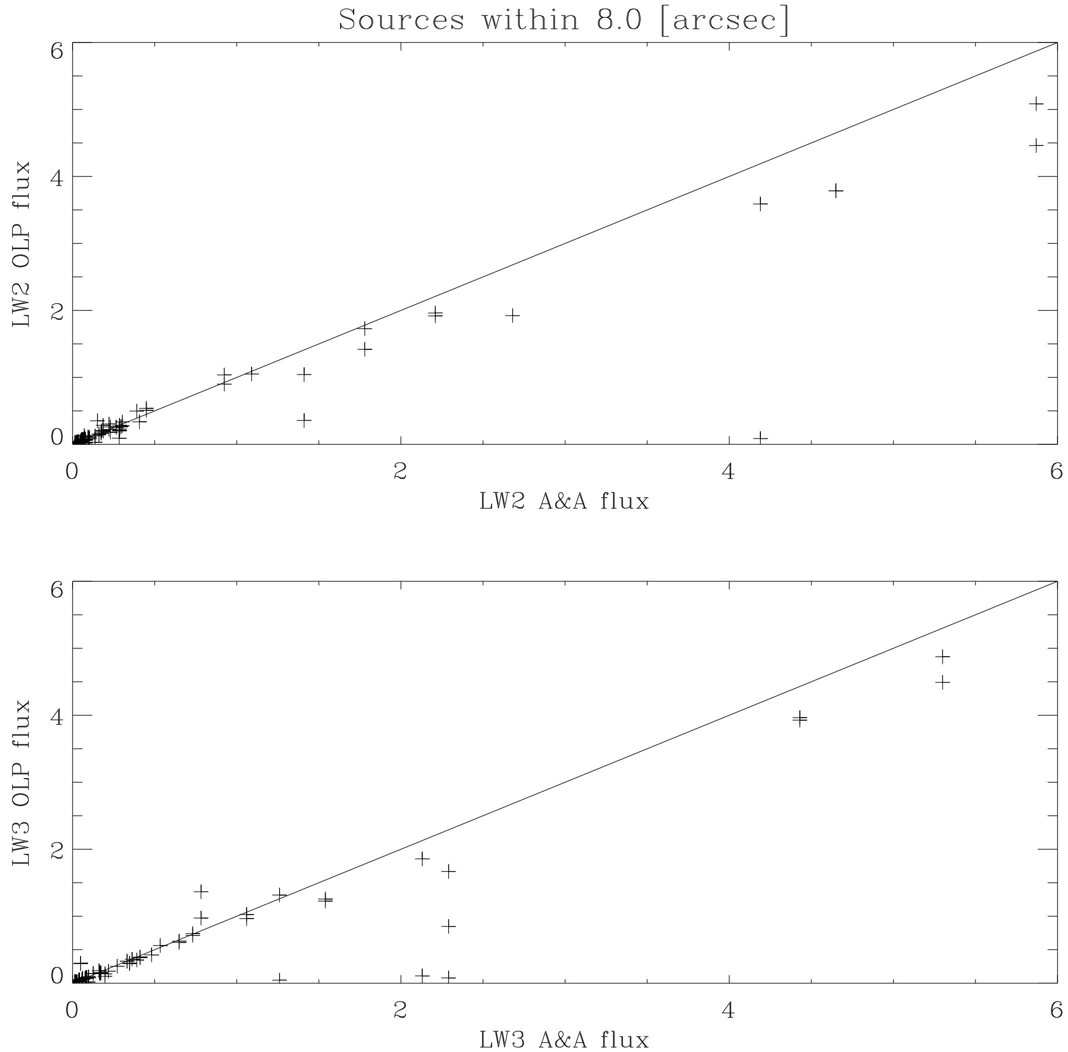

Figure 24: Fluxes of point sources in ρ Oph found by OLP and obtained from the hand–reduction of A&A.

- As indicated in the CAM cookbook, straylight generated ghosts can lead to spurious extended features within the data. Ghosts seem to affect mainly CVF data, at any field of view other than 1.5 arcsec.
- Lens- and filter- wheel jitter can lead to imperfect flat–fielding at the edges of CMAPs, where Flux errors up to a factor of 5 may occur.
- In case of SW observations of a strong source the dark current may be overestimated, which leads to an apparent negative background.

8.3.3 CMOS products

Since CMOS are created from CMAPs, all the caveats above apply. Note some further caveats:

- AAC performs photometry on CMAP sources, i.e. before mosaic reconstruction. Hence faint sources, visible only after mosaic reconstruction, will have escaped detection by AAC's photometric module and may, in extreme cases, not be visible in the CMAPs.

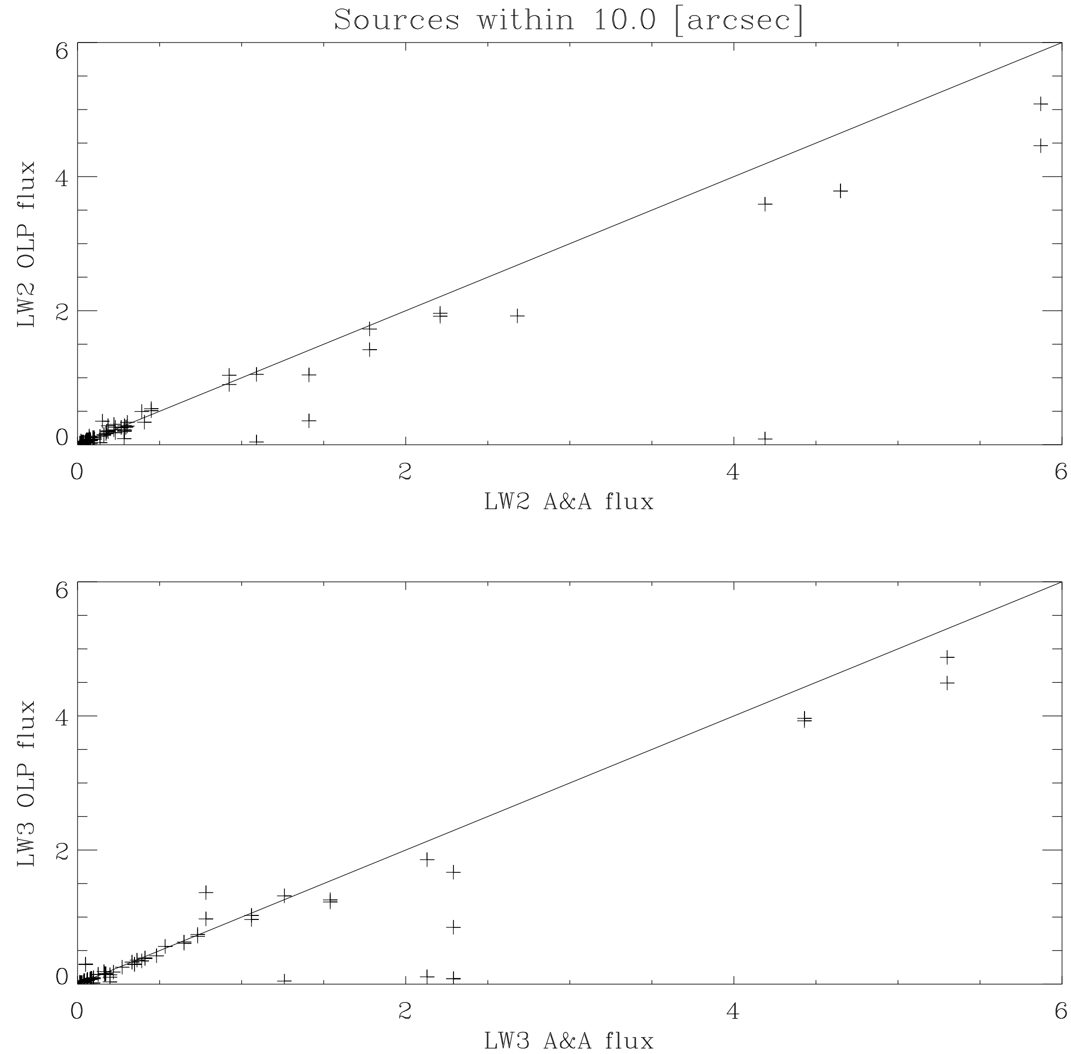

Figure 25: Fluxes of point sources in ρ Oph found by OLP and obtained from the hand–reduction of A&A.

- Upon constructing mosaics from CMAPs, optical field distorsion is not taken into account. This may lead to "blurred" point sources.

8.3.4 CPSL

Despite the Flux uncertainty reported in CPSL – which is a statistical error value – Flux values are believed to be subjected to a systematic underestimation of some 5–15 % in most cases. The reason is believed to be due to the different Fluxes obtained by PSF fitting (as AAC does) and aperture photometry (as used to derive the calibration files). The corolary is that manual aperture photometry applied to AAC data products should yield a more precise photometry than found by AAC.

This holds also true for polarization observations done with LW2, LW3, LW7, LW9 and LW10. For polarization observations done with other filters, as a first order approximation, the Flux has to be augmented by 20%.

It should be noted that AAC performs photometry on CMAP sources, i.e. previous to mosaic reconstruction. Hence faint sources, visible only after mosaic reconstruction, will have escaped detection by AAC's photometric module.

- Wavelengths and Fluxes near the extreme wavelength end ranges of the CVF range are unreliable.
- Lens- and filter- wheel jitter can introduce spurious point sources in CPSL.
- For a variety of calibration and algorithmic related causes the point–source detection algorithm is prone to find some spurious sources for the SW detector or around strong gradients.
- As there are no corrections for varying CVF wavelength across the detector, off–axis sources suffer a wavelength shift that may amount to the equivalent of one CVF step.
- Unrecognized glitches may be mistaken as sources.
- Astrometry is subject to the following errors :
    - No corrections are available yet for the variation of ISOCAM's optical axis as a function of filter (up to 2 arcsec), CVF position (up to 6 arcsec from one LW segment to the other) and for LW/SW separation (SW images are displaced -6 arcsec (Y–direction) and -3 arcsec (Z–direction) with respect to LW images. In extreme cases, a celestial source detected at one wavelength may be "re–detected" with different RA, DEC at other wavelengths.
    - No corrections are made for optical distortion (up to one pixel).
    - No corrections are made for lens wheel repositioning jitter; the error may amount to the equivalent of one to two pixels across the detector "columns" direction (it is simple to recognize the columns since column 24 connection was broken during satellite integration and it appears as a dark line in several images.)
    - The point source detection algorithm resamples data to a 1/3 of a pixel. Hence astrometry cannot be more precise than 1/3rd of the Pixel Field of View.

8.3.5 CSSP files

AAC collates spectral information for those sources listed in CPSL, so all the CPSL caveats apply here as well. In particular, the same source which is detected twice or more at apparently different positions in different filters will correspondingly give rise to two or more spectra.

8.3.6 CUFF

Flux error estimates reported in CUFF are statistical values and do not take into account systematic effects. Indicated average Fluxes pertaining to CMAPs are reliable except for the end range of CVFs and in case of SW observations with a strong point source.

8.3.7 CJAM and CGLL files

CJAM and CGLL contain auxiliary information. The contents of CGLL has been verified and it is reliable.

A Figures for Section 6

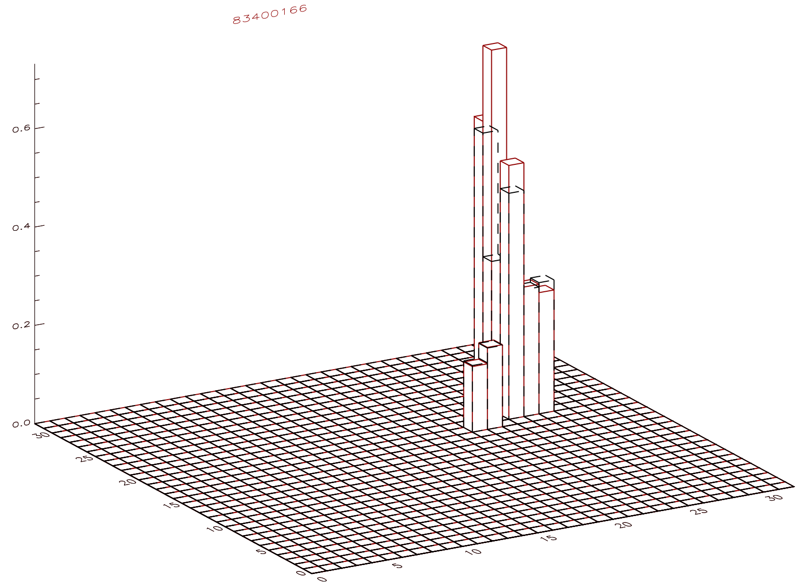

Figure 26: Point sources found for cpsl83400166. This and the following similar plots use solid lines for memory corrected data and dashed line for uncorrected data.

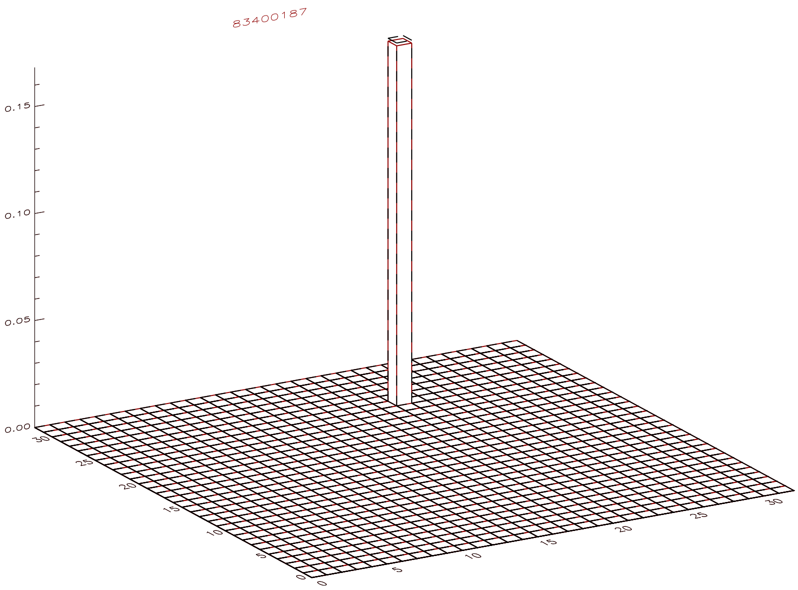

Figure 27: Point sources found for cpsl83400187

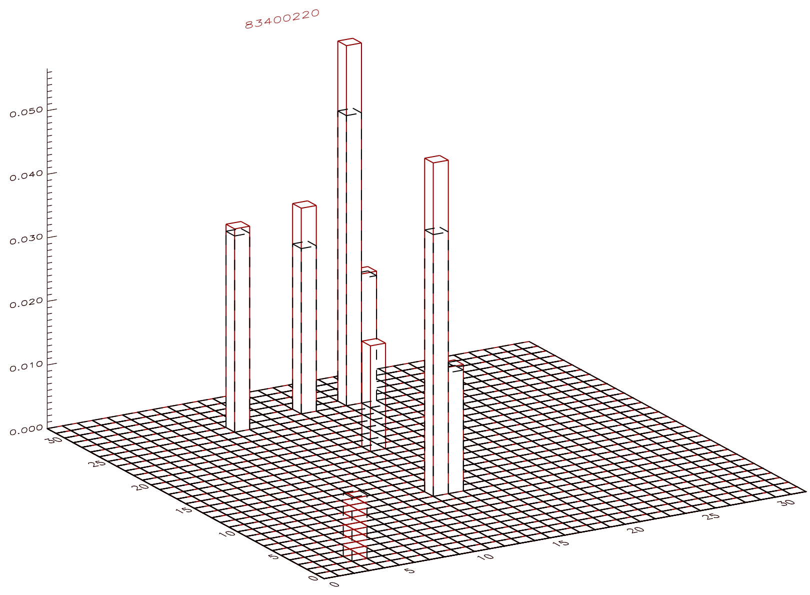

Figure 28: Point sources found for cpsl83400220

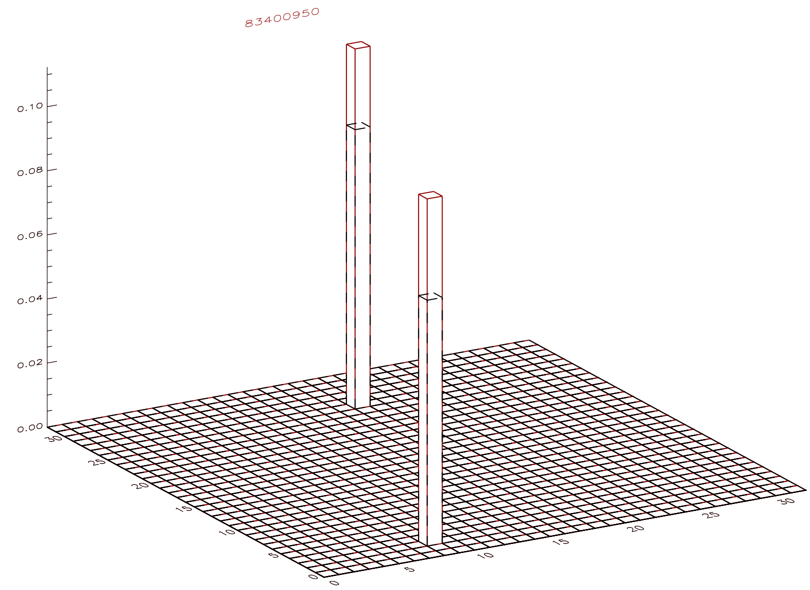

Figure 29: Point sources found for cpsl83400950

Dos

A TDTs used in the validation exercise

01100101 01402705 01402901 01500101 01500808 01501209 01801102 03000102
03000502 03000704 03000906 03001108 03001209 03001411 03001613 03001714

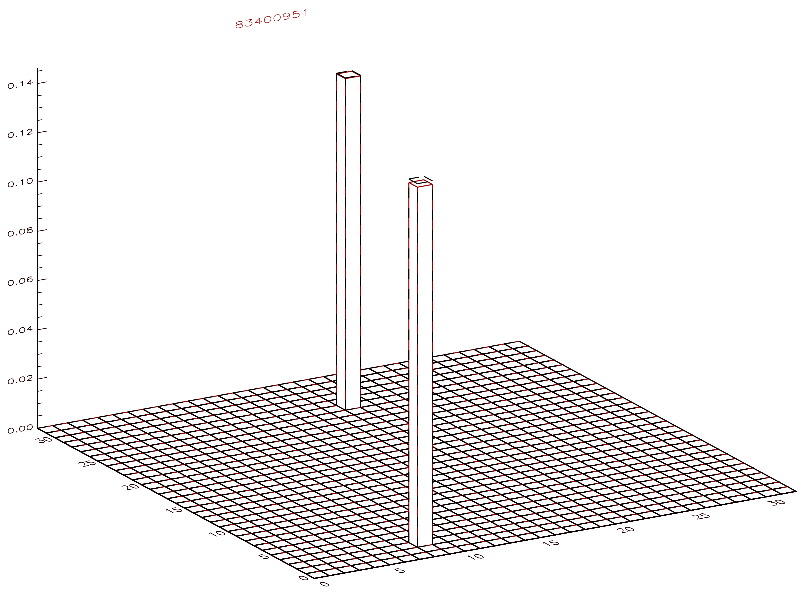

Figure 30: Point sources found for cpsl83400951

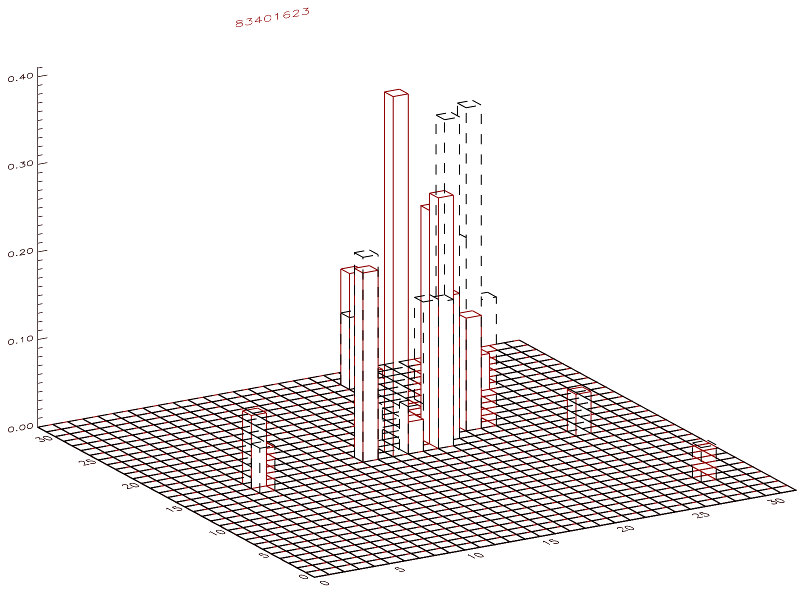

Figure 31: Point sources found for cpsl83401623

03001815 03001916 03002017 03002219 03002421 03002522 03002623 03002825
03003027 03003128 03003229 03003401 03003502 03400802 03401004 03401206
03401408 03401509 03401711 03401913 03402014 03402115 03402216 03402317
03402519 03402721 03402822 03402923 03403125 03403327 03403428 03403529
03403731 03403832 03403933 03404034 03404135 03404236 03404337 03404438
03404539 03404640 03404741 03404901 03405002 03405103 03805455 03805556
03805657 03805758 03805859 03805960 04200403 04600304 04603506 04603708

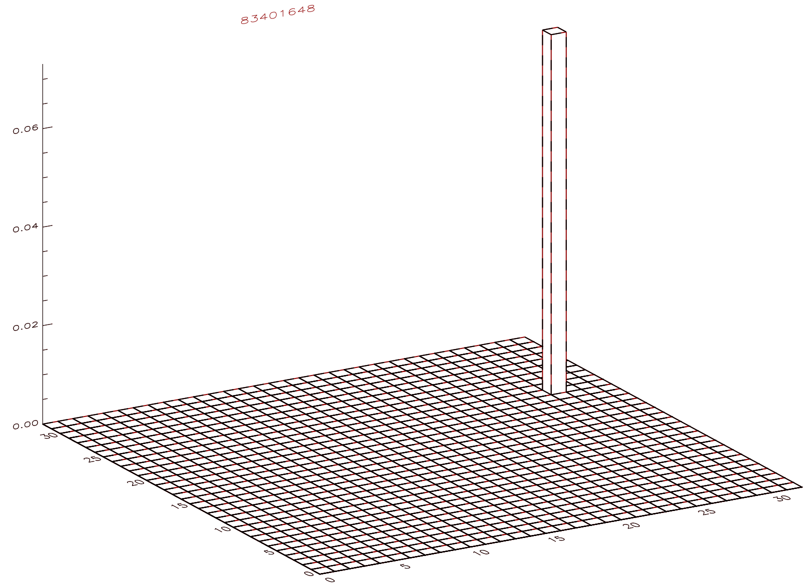

Figure 32: Point sources found for cpsl83401648

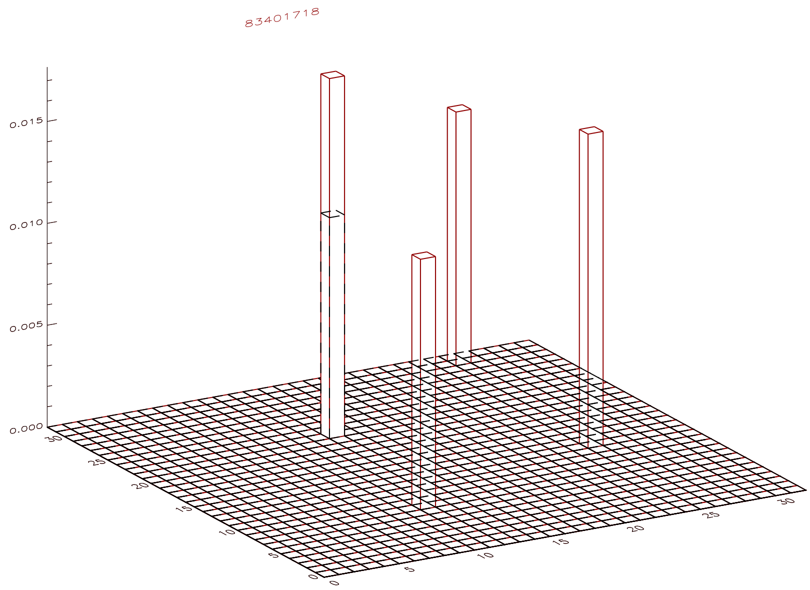

Figure 33: Point sources found for cpsl83401718

04603809 05400564 05400665 05400766 05400867 05400968 05401069 05401323
05401424 05401525 05401626 05402029 05402130 05402231 05402332 05402635
05402736 05402837 05402938 05804802 05804903 05805004 05805408 05805509
05805610 06202141 06202242 06202343 06203408 06603207 06701012 06701113
07801201 07807002 08500618 08502329 08602601 08604502 08901903 08902411
09002501 09101820 09101925 09700453 09700621 09800201 09800435 09800438
09800523 09800526 09800612 09800613 09800827 09800828 09800830 09800831

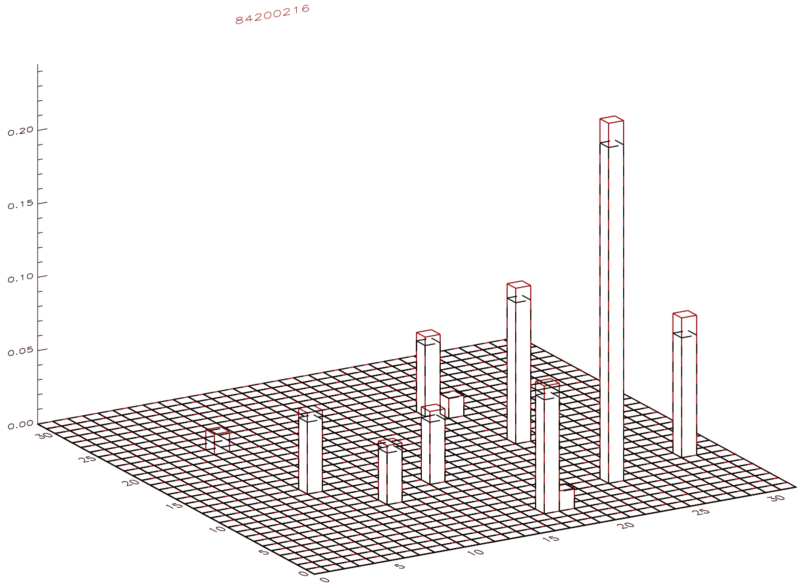

Figure 34: Point sources found for cpsl84200216

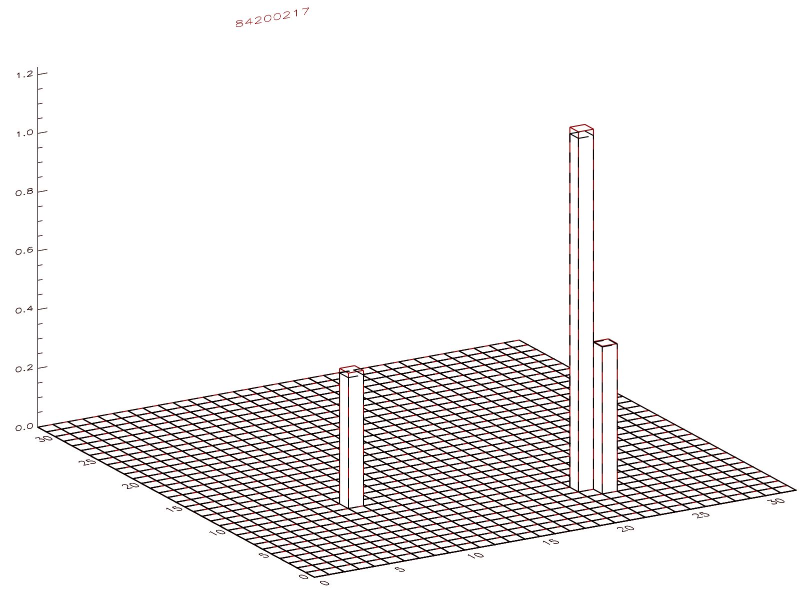

Figure 35: Point sources found for cpsl84200217

09800977 09801015 09801016 09801129 09801132 09801217 09801218 10100122
10100622 10380100 10402702 10602912 10603407 10702605 12401910 12700714
12701535 13000104 13305901 13306013 13580800 14704905 15201210 16300605
16803908 16804009 16804114 16804215 16804316 16804417 17503636 19000909
19000910 23300257 25000152 25000204 25000303 25001211 25102703 25301301
26101501 27300704 28792300 30100907 30201662 30800215 31201608 31500511
31601707 32201212 32201536 32201615 32201830 32201917 32500256 32500354

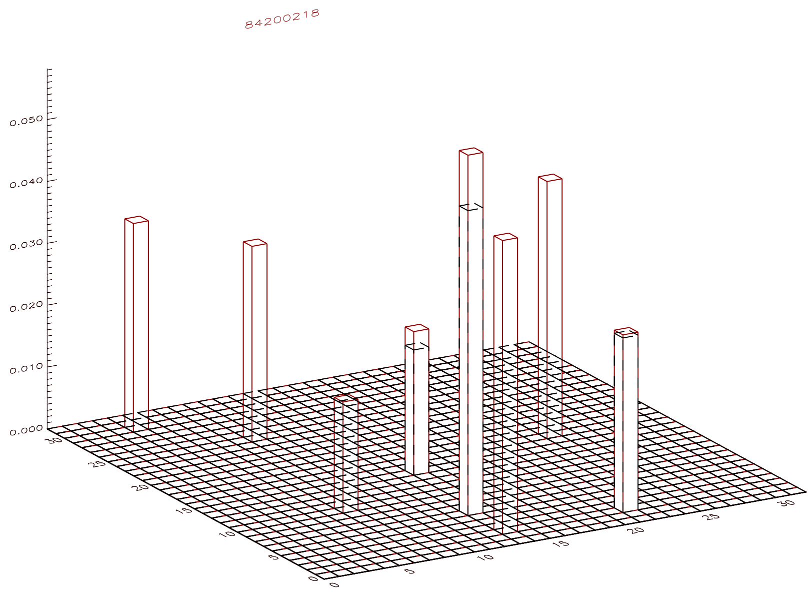

Figure 36: Point sources found for cpsl84200218

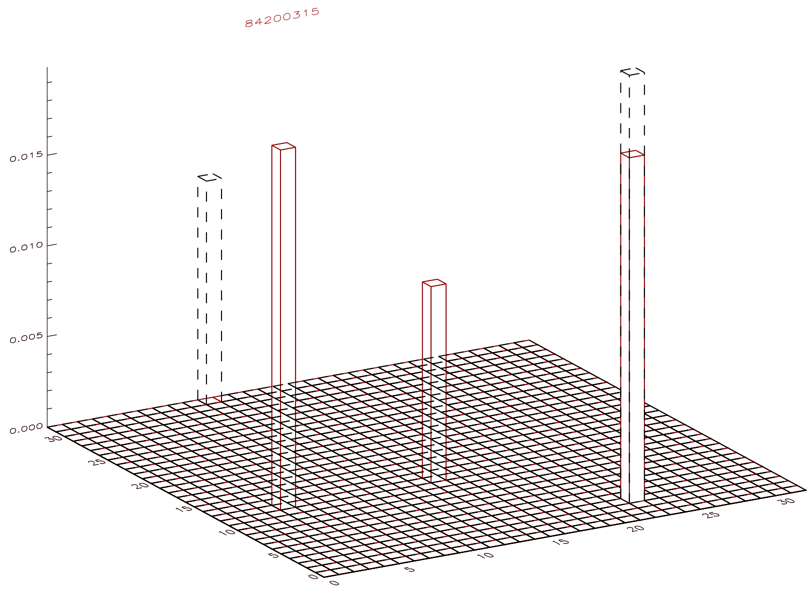

Figure 37: Point sources found for cpsl84200315

32880600	33101303	33480500	34301519	34901401	35600401	35600501	36500551
36700802	37703603	38602744	39102702	39103002	39103503	39104008	39104701
39104801	41204803	41900718	41900819	41900920	41901021	41901122	41902105
41902206	41902307	41902408	41902509	41902610	41902711	41902812	41902913
41903023	41903124	41903252	41903353	41903454	41903555	41903656	41903757
41903858	41903959	41904060	41904262	41904363	41904464	41904565	41904666
41904767	41904868	41904969	42902940	45001101	45001101	45001201	45001201

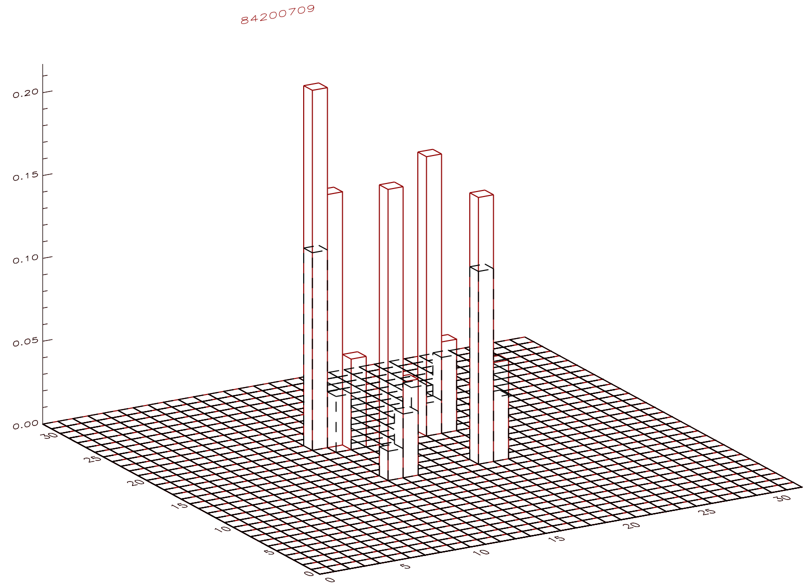

Figure 38: Point sources found for cpsl84200709

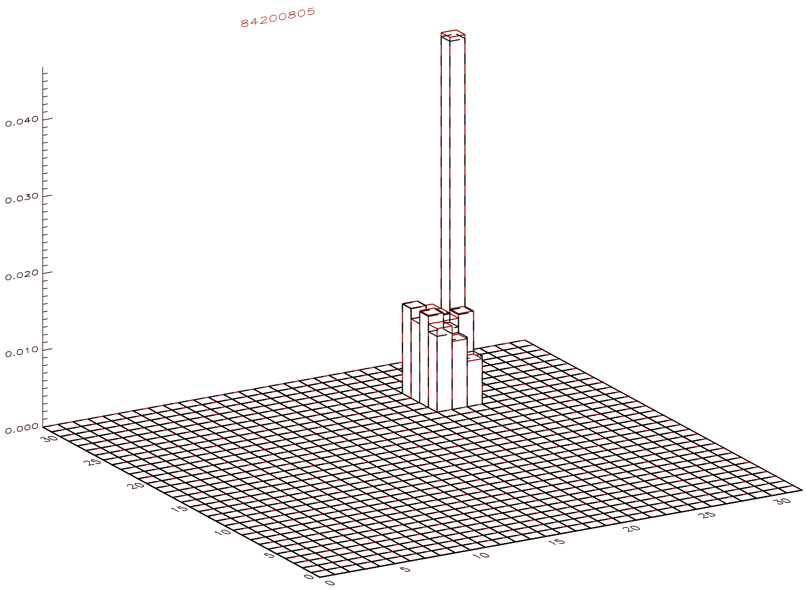

Figure 39: Point sources found for cpsl84200805

45001301 45001301 45501431 45800955 46001722 46600901 46601001 46601201
46702001 46702101 46702201 46900501 46900601 48401245 48700810 48780200
48801335 49100301 49100301 49701770 50200301 50304201 50501608 51200301
51700403 52080700 54101418 54700407 55200707 55200808 55200909 55201010
55201111 55201212 55201313 55201414 55201515 55201616 55202020 55202121
55202222 55202323 55202727 55202828 55202929 55203030 55203636 55203737
55203838 55203939 55204040 55204141 55204242 55204343 55204444 55204545

55302308 55380100 56300113 57200101 57502001 60200101 60200220 60292300
60701040 61092300 61700101 61782200 62581400 62600101 62692300 63003362
63201101 63901114 64792300 64801324 65500701 65501004 65501105 65581500
66200201 66200302 66200403 66200504 66200605 66200706 66200807 66200908
66201009 66201113 66201214 66201315 66201416 66201517 66201618 66201719
66201820 66201921 66202022 66202123 66202224 66202325 66202426 66202527
66202628 66202729 66202830 66202931 66203032 66203133 66203234 66203335
66203436 66203537 66203638 66203739 66203840 66203941 66204042 66204143
66280400 66801791 67401402 69602208 70700101 70700202 70700303 70700404
70700505 70700606 70700707 70700801 70700902 70701003 70701104 70701205
70701306 70701407 70701501 70701602 70701703 70701804 70701905 70702006
70702107 70702201 70702302 70702403 70702504 70702605 70702706 70702807
70702901 70703002 70703103 70703204 70703305 70703406 70703507 70703601
70703702 70703803 70703904 70704005 70704106 70704207 70796100 70796200
70796300 71501017 71580800 75100202 76100807 76780600 77604505 77780400
77801401 79100204 79100305 79100506 80803012 83300401 83401623 84602202
84902275 85900401 87002103